QCD phase structure under rotation and acceleration

Xu-Guang Huang

Fudan University, Shanghai

Second International Workshop on Physics at High Baryon Density
October 16, 2025 @ CCNU, Wuhan

Content

- Introduction
  Why acceleration and rotation are interesting for quark matter study

- Rotational effect on QCD phase structure
  Models versus lattice results

- Acceleration effects on QCD phase structure
  Models versus lattice results

- Summary

Introduction

Where is accelerating and rotating QCD matter

- A typical example is quark gluon matter in heavy-ion collisions

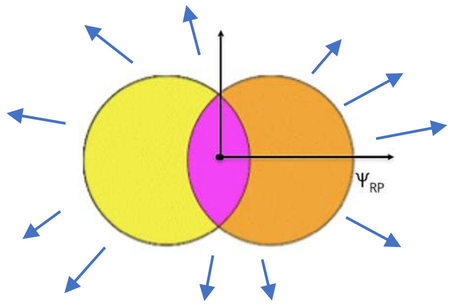

$$\boldsymbol{a} = \frac{d\boldsymbol{v}}{dt} = -\frac{1}{\varepsilon + P}\boldsymbol{\nabla} P$$

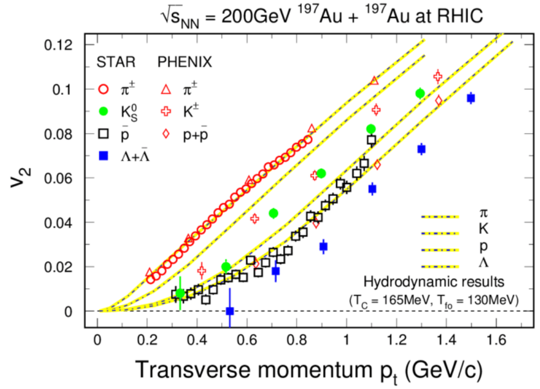

Elliptic flow due to fluid acceleration

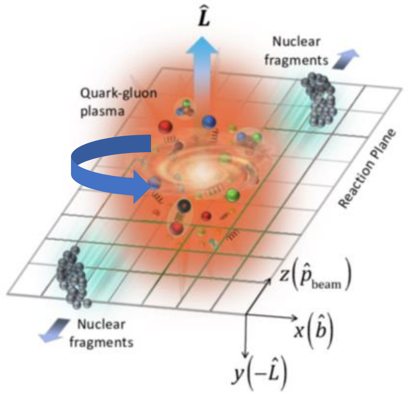

$$\boldsymbol{\Omega} = \frac{1}{2}\boldsymbol{\nabla} \times \boldsymbol{v}$$

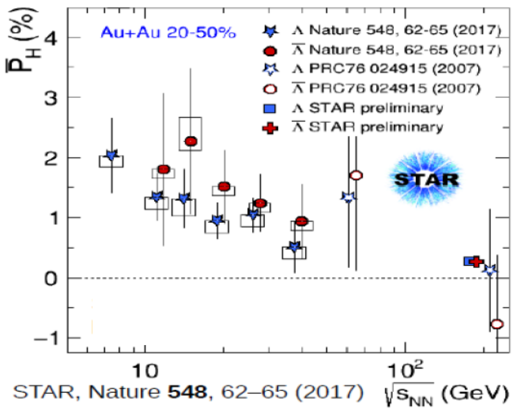

Spin polarization due to fluid rotation (vorticity)

Effect of rotation: Comparison with chemical potential

- Hints for possible rotation effect: comparison with chemical potential

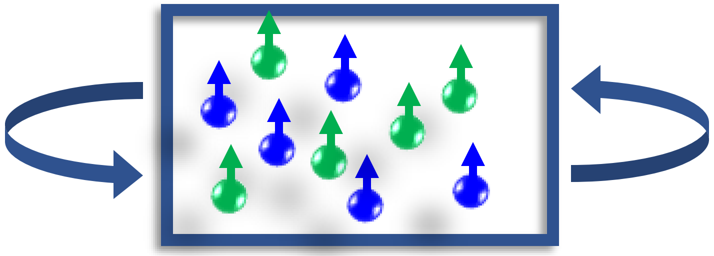

Rotation

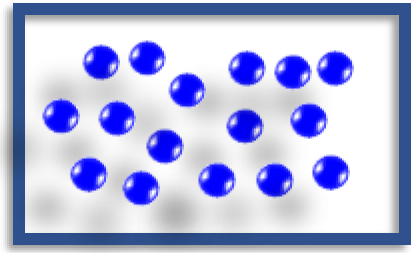

Chemical potential

$$H = H_0 - \Omega J_z$$

$$H = H_0 - \mu N$$

For massless Dirac fermions

$$P = \frac{7\pi^2}{180\beta^4} + \frac{(\Omega/2)^2}{6\beta^2} + \frac{(\Omega/2)^4}{12\pi^2}$$

(At rotating axis, for unbounded system)

$$P = \frac{7\pi^2}{180\beta^4} + \frac{\mu^2}{6\beta^2} + \frac{\mu^4}{12\pi^2}$$

(Ambrus and Winstanley 2019; Palermo etal 2021)

>>> Both have sign problem on lattice

Effect of acceleration: Comparison with chemical potential

- Hints for possible acceleration effect: comparison with chemical potential

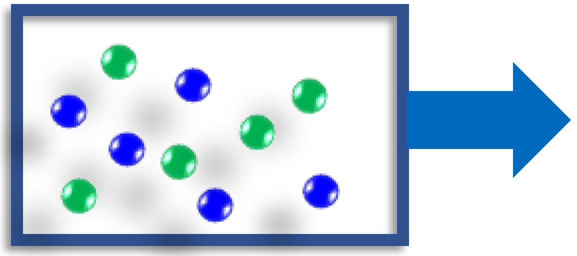

Acceleration

$$H = H_0 - aK_z$$

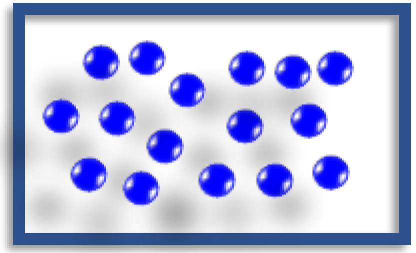

Chemical potential

$$H = H_0 - \mu N$$

For massless Dirac fermions

$$P = \frac{7\pi^2}{180\beta^4} + \frac{(a/\sqrt{12})^2}{6\beta^2} - \frac{17}{20}\frac{(a/\sqrt{12})^4}{12\pi^2}$$

$$P = \frac{7\pi^2}{180\beta^4} + \frac{\mu^2}{6\beta^2} + \frac{\mu^4}{12\pi^2}$$

(Prokhorov etal 2019; Palermo etal 2021)

>>> Sign problem for acceleration can be avoided

Accelerating and rotating thermal equilibrium

- Many-body system can remain equilibrium with acceleration and rotation
- Local equilibrium (LE) density operator

$$\rho_{\mathrm{LE}} = \frac{1}{Z_{\mathrm{LE}}} \exp\left[-\int d\Xi_\mu \left(T^{\mu\nu}\beta_\nu - \frac{1}{2} J^{\mu\rho\sigma}\varpi_{\rho\sigma} \right) \right]$$

- True global equilibrium ρ_{eq} is a time-independent LE

$$\Rightarrow \quad \beta^\mu \text{ and } \varpi^{\mu\nu} \text{ are constants}$$

$$\left\{ \begin{aligned} \beta^\mu &= (\beta, \mathbf{0}) \\ \varpi_{0i} &= \beta a^i \\ \varpi_{ij} &= \beta \epsilon^{ijk}\Omega^k \end{aligned} \right. \quad \Rightarrow \quad \rho_{\mathrm{eq}} = \frac{1}{Z_{\mathrm{eq}}} \exp\left[-\beta \left(H - \boldsymbol{a}\cdot\boldsymbol{K} - \boldsymbol{\Omega}\cdot\boldsymbol{J} \right) \right]$$

Boost operator

Angular momentum

QCD phase diagram

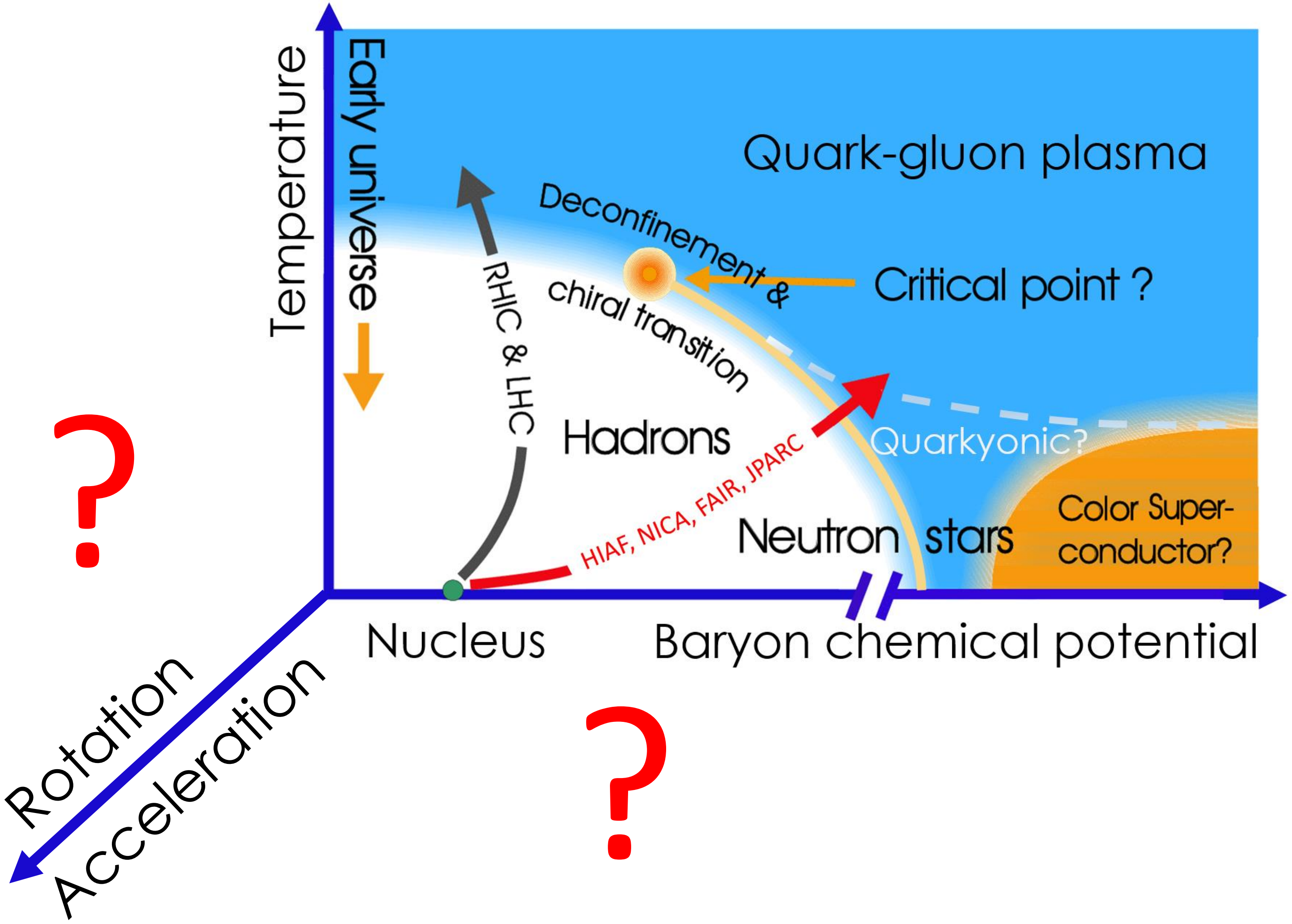

- Chiral condensate and confinement?
- Effects combined with finite B field, densities, … ?
- Possible signatures in HICs?

Rotational effects

Angular momentum polarization

- Consider a scalar (or pseudoscalar) pair of fermions

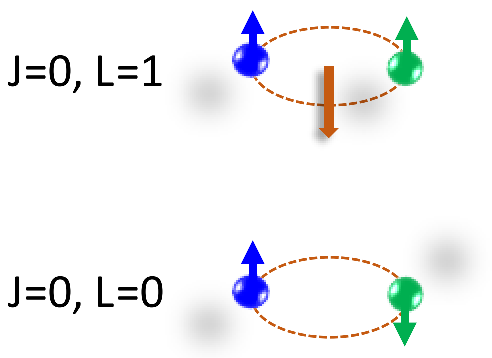

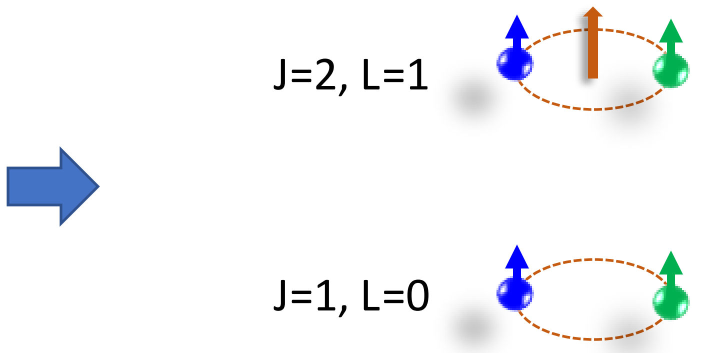

- Thus in general, one expects that rotation tends to suppress $\sigma, \pi, \ldots \ldots$
- Compare with magnetic catalysis (dimensional reduction)

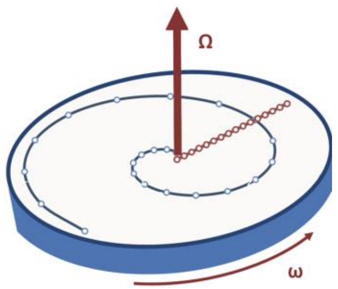

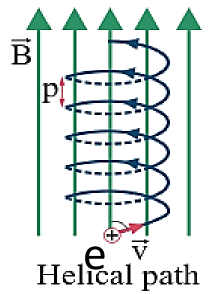

Rotating fermions

- Let us consider fermions; bosons can be similarly discussed.
- Consider a rotating frame

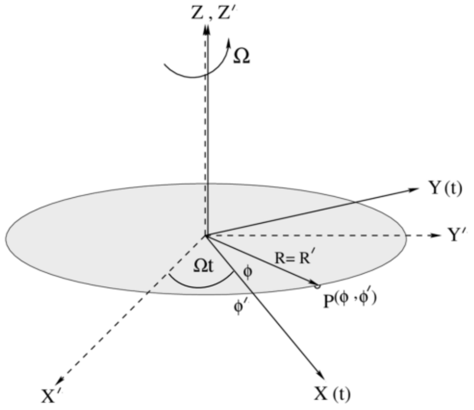

$$\begin{cases} x' = x\cos\Omega t - y\sin\Omega t \\ y' = x\sin\Omega t + y\cos\Omega t \\ z' = z \\ t' = t \end{cases} \quad \Rightarrow \quad g_{\mu\nu} = \begin{pmatrix} 1-\Omega^2 r^2 & \Omega y & -\Omega x & 0 \\ \Omega y & -1 & 0 & 0 \\ -\Omega x & 0 & -1 & 0 \\ 0 & 0 & 0 & -1 \end{pmatrix}$$

- Fermion field

$$S = \int d^4x \sqrt{-g}\,\bar{\psi}\left(i\gamma^\mu \nabla_\mu - m_0\right)\psi \qquad \nabla_\mu = \partial_\mu + i\hat{Q}A_\mu + \Gamma_\mu$$

$$\Downarrow$$

$$H = \hat{Q}A_0 + m_0\beta + \boldsymbol{\alpha}\cdot\boldsymbol{\pi} - \boxed{\boldsymbol{\Omega}\cdot(\mathbf{r}\times\boldsymbol{\pi} + \boldsymbol{\Sigma})}$$

Rotating fermions

- Uniformly rotating system must be finite

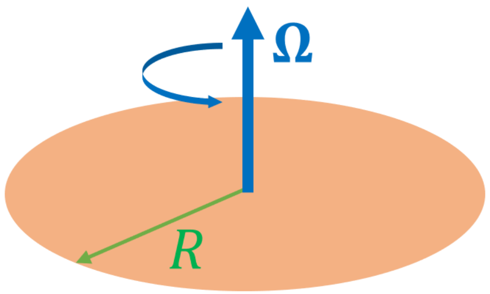

$$\boldsymbol{\Omega R \leq 1}$$

- Boundary conditions for Dirac fermions in a cylinder
  - Dirichlet B.C. (No)
  - MIT B.C. (Yes)

$$[i\gamma^{\mu} n_{\mu}(\theta) - 1]\psi\Big|_{r=R} = 0 \quad \Rightarrow \quad j^{\mu} n_{\mu} = 0 \quad \text{at} \quad r = R$$

  - No-flux B.C. (Yes)

$$\int d\theta \bar{\psi} \gamma^{r} \psi \Big|_{r=R} = 0 \quad \Rightarrow \quad \text{Minimum request for Hermiticity}$$

(Ambrus-Winstanley 2015, Ebihara-Fukushima-Mameda 2016, Chen etal 2017, Chernodub-Gongyo 2016-2017)

Rotating fermions

- Consider no-flux B.C.

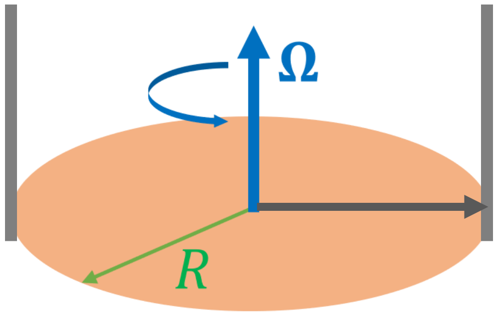

- $p_t = p_{l,k}$ discretized by $J_l(p_{l,k}R) = 0$
- $E = (p_{l,k}^2 + p_z^2 + m^2)^{1/2} > \Omega|l + \frac{1}{2}|$
- Vacuum does not rotate

(Vilenkin 1979, Ambrus-Winstanley 2015,Ebihara-Fukushima-Mameda 2016)

- To see uniform rotation effect, we need $\boldsymbol{T}$, $\boldsymbol{\mu}$, $\boldsymbol{B}$, ……

Figures drawn by K.Mameda

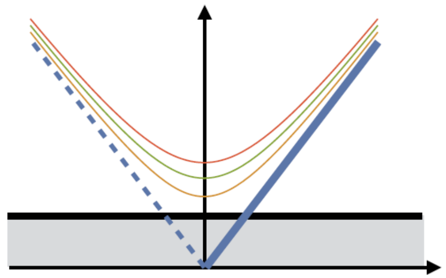

B: Chen etal 2015, Liu-Zahed 2017,Chen-Mameda-XGH 2019, Cao-He 2019, Tabatabaee etal 2021, Eto-Nishimura-Nitta 2023, etal 2023, Kiefer-Dash-Rischke 2025, …

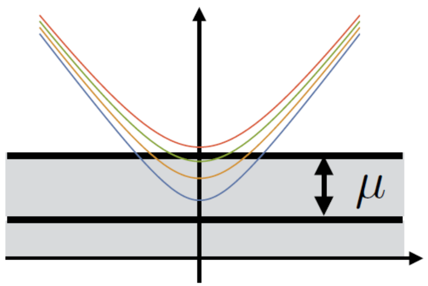

μ: XGH-Nishimura-Yamamoto 2017, Zhang-Hou-Liao 2018, Huang etal 2018, Nishimura etal 2020,2021, Morales-Tejera etal 2025, …

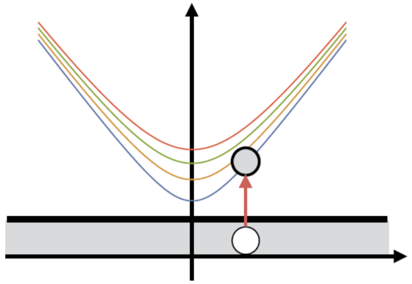

T: Jiang-Liao 2016, Chernodub-Gongyo 2017, Wang etal 2019, Luo etal 2020, Jiang 2021, Cheb-Zhu-XGH 2023, Sun etal 2024, …

Rotating Nambu-Jona-Lasinio model

- Take a four-fermion model

$$Z = \int \mathcal{D}[\bar{\psi}, \psi] \exp\left(i \int d^4x \sqrt{-g} \mathcal{L}_{\mathrm{NJL}} \right)$$

$$\mathcal{L}_{\mathrm{NJL}} = \bar{\psi}(i\gamma^\mu \nabla_\mu - m_0)\psi + \frac{G}{2}[(\bar{\psi}\psi)^2 + (\bar{\psi} i \gamma^5 \boldsymbol{\tau} \psi)^2]$$

$$\nabla_\mu = \partial_\mu + i\hat{Q} A_\mu + \Gamma_\mu$$

- Mean-field approximation

$$V_{\mathrm{eff}} = \frac{1}{\beta V} \int d^4 x_E \left\{ \frac{\sigma^2 + \boldsymbol{\pi}^2}{2G} - \sum_{\{\xi\}} \left[\frac{\varepsilon_{\{\xi\}}}{2} + \frac{1}{\beta} \ln(1 + e^{-\beta \varepsilon_{\{\xi\}}}) \right] \Psi^\dagger_{\{\xi\}} \Psi_{\{\xi\}} \right\}$$

$\varepsilon_{\{\xi\}}$ and $\Psi_{\{\xi\}}$: Eigen-energy and eigen-wavefunction with quantum numbers $\{\xi\}$

Rotating Nambu-Jona-Lasinio model

- Consider a simple case: massless, no pion modes, homogeneous

$$\varepsilon_{l,\pm} = \pm\sqrt{p_z^2 + p_t^2 + \sigma^2} - \Omega\left(l + \frac{1}{2}\right)$$

Ration

$$\varepsilon_{n,\pm} = \pm\sqrt{p_z^2 + \sigma^2 + 2nqB}$$

Magnetic field

- Chiral condensate vs rotation and/or magnetic field

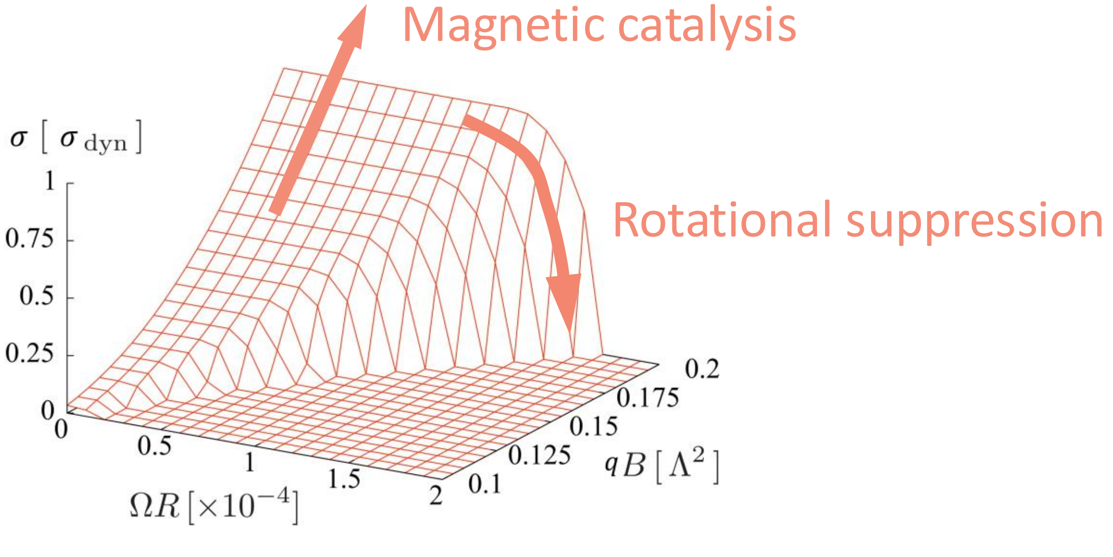

$G < G_c$

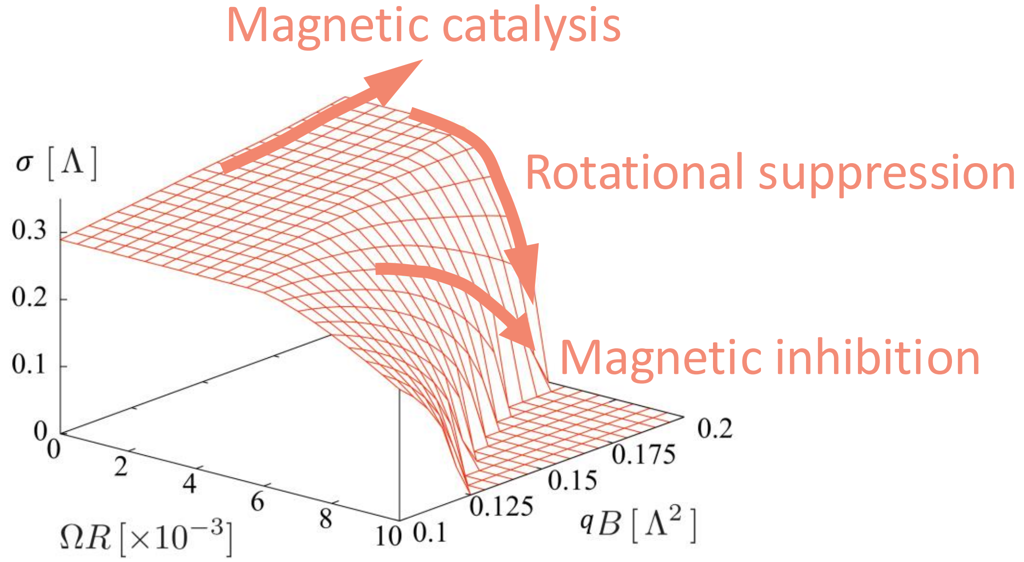

$G > G_c$

(Chen-Fukushima-XGH-Mameda 2015)

Rotating Nambu-Jona-Lasinio model

- Consider a simple case: massless, no pion modes, homogeneous

$$\varepsilon_{l,\pm} = \pm\sqrt{p_z^2 + p_t^2 + \sigma^2} - \boxed{\Omega\left(l + \frac{1}{2}\right)}$$

μ

Ration

$$\varepsilon_{n,\pm} = \pm\sqrt{p_z^2 + \sigma^2 + 2nqB}$$

Magnetic field

- Compare with finite-density case:

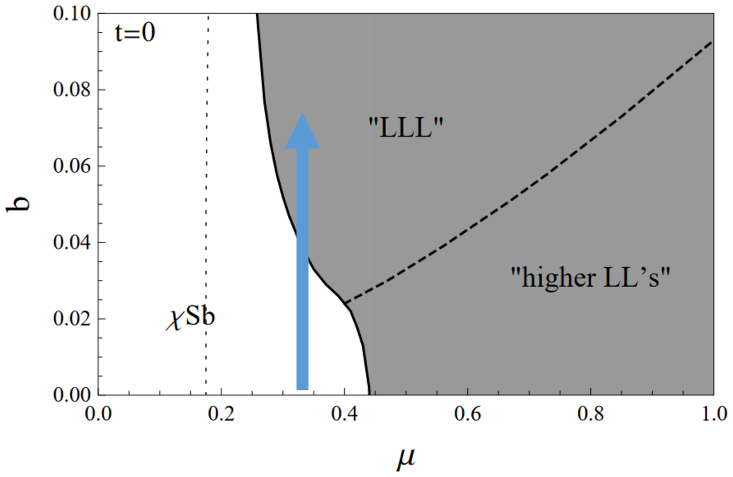

Sakai-Sugimoto model

(Freis-Rebhan-Schmitt 2010)

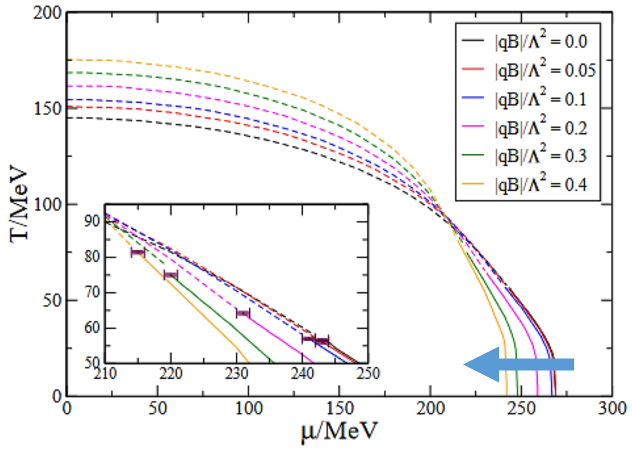

Quark-meson model

(Andersen-Tranberg 2012)

Rotating Nambu-Jona-Lasinio model

- Many mean-field studies support rotation suppresses chiral condensate. E.g.:

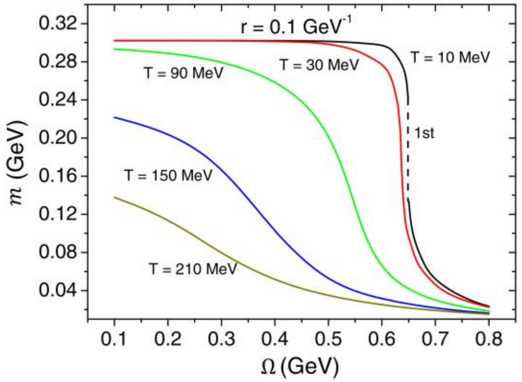

(Jiang-Liao 2016)

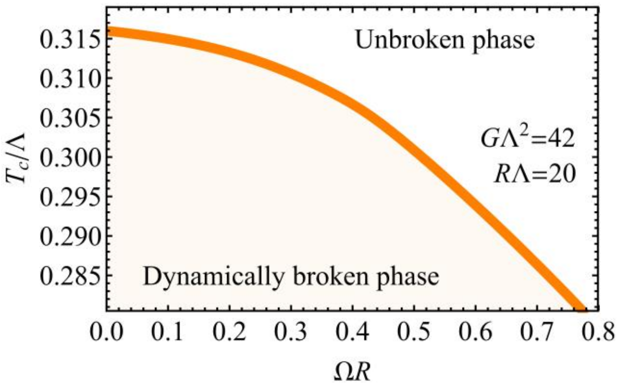

(Chernodub-Gongyo 2016)

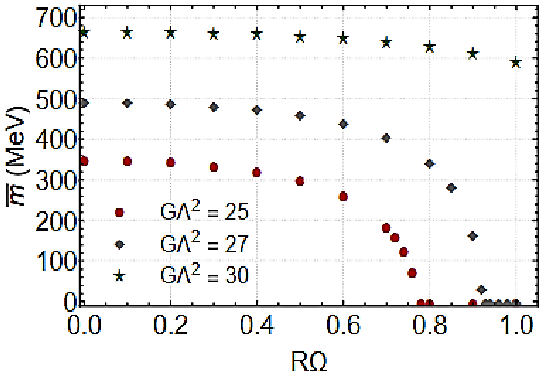

(Sadooghi-Mehr-Taghinavaz 2022)

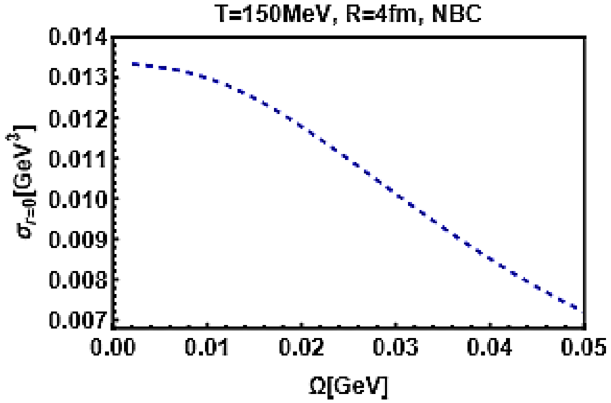

(Chen-Li-Huang 2022)

Formulate rotating lattice

- Gluons and Wilson fermions (Angular momentum) (Yamamoto-Hirono 2013)
- Pure gluons (Polyakov loop) (Braguta etal 2021)
- We consider gluons and 2+1 flavor staggered fermions

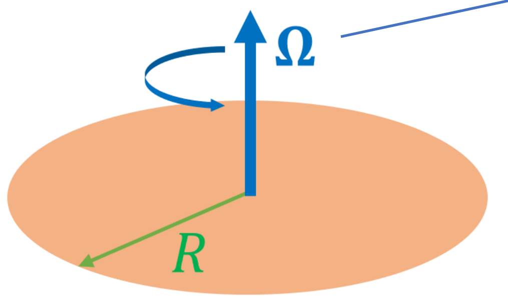

Imaginary rotation: $\boldsymbol{\Omega \to -i\Omega_I}$

No sign problem
No causality constraint

Projective-plane B.C for x-y plane
Periodic B.C. for t and z direction

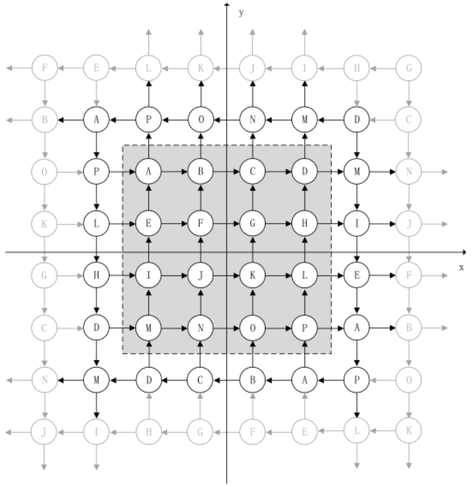

- We measure: chiral condensate and Polyakov loop

$$\Delta_{l,s}(T,\Omega_I) = \frac{\langle\bar{\psi}_l\psi_l\rangle_{T,\Omega_I} - \frac{m_l}{m_s}\langle\bar{\psi}_s\psi_s\rangle_{T,0}}{\langle\bar{\psi}_l\psi_l\rangle_{0,0} - \frac{m_l}{m_s}\langle\bar{\psi}_s\psi_s\rangle_{0,0}}$$

$$L_{\mathrm{ren}} = \exp(-N_\tau c(\beta)a/2)L_{\mathrm{bare}}$$

$$L_{\mathrm{bare}} = \left|\mathrm{tr}\left[\sum_{\mathbf{n}}\prod_\tau U_\tau(\mathbf{n},\tau)\right]\right|/3N_x^3$$

Results for chiral condensate

- Chiral condensate and chiral susceptibility

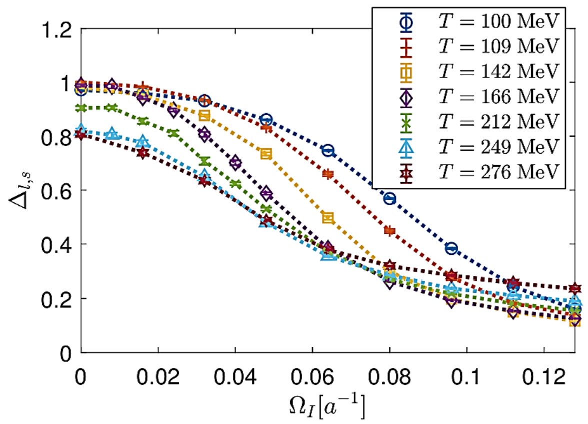

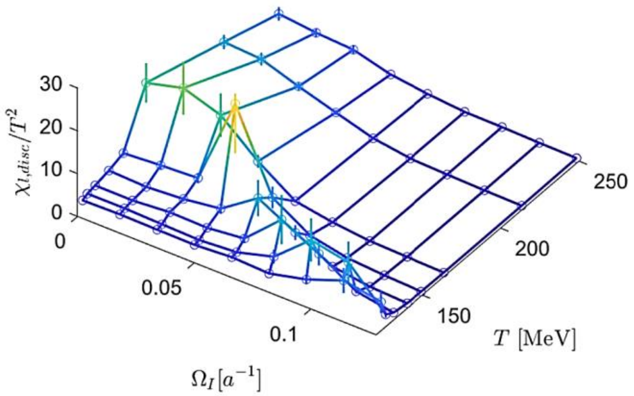

- Analytical continuation to real rotation $\Omega_I \rightarrow i\Omega$

Chiral condensate must be even function of Ω

Chiral condensate increase with real Ω!

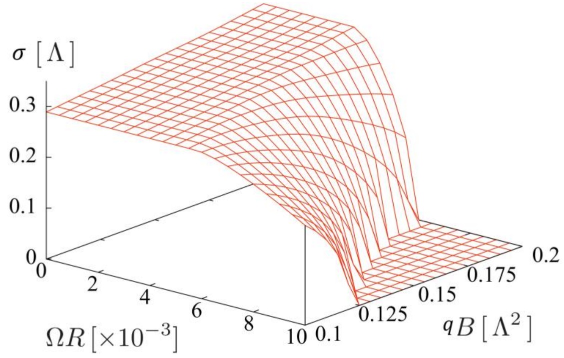

Recall e.g mean-field results for NJL model

Sharp conflict between effective models and lattice!

Results for Polyakov loop

- Polyakov loop and its susceptibility: Real rotation catalyze quark confinement

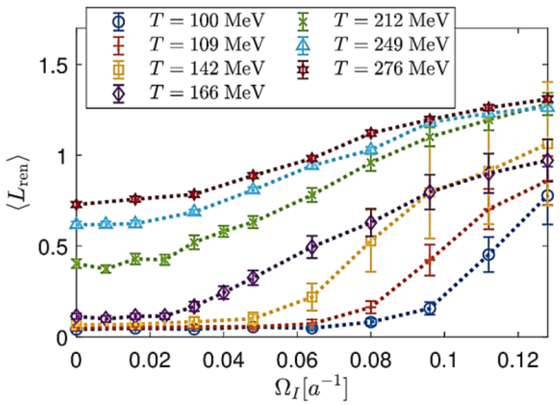

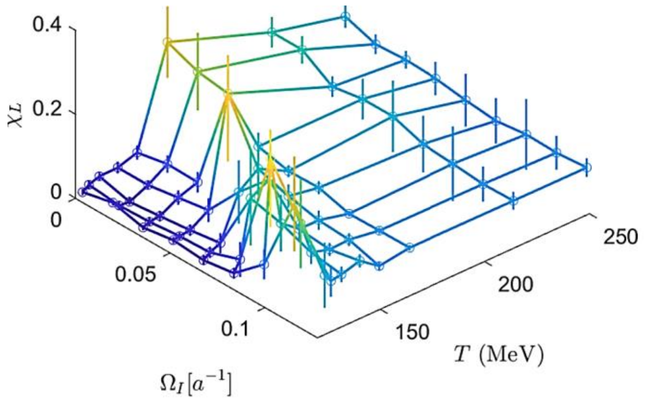

- ~~Pseudo-critical~~ temperature ~~decreases~~ due to ~~imaginary~~ rotation

Critical increases real

- Consistent with previous pure gluon simulation

(Braguta etal 2021)

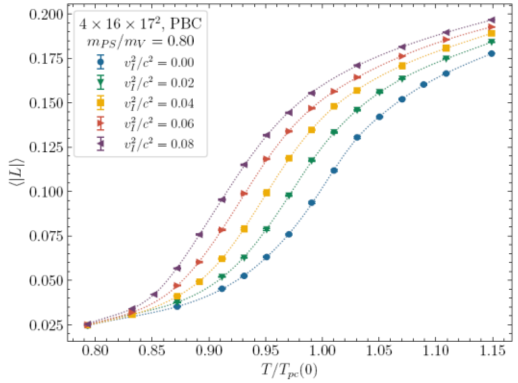

Contradict with model studies, not understood too

Acceleration effects

Accelerating frame and Rindler coordinates

- An observer with constant proper acceleration in Minkowski spacetime

$$t_M^2 - \left(z_M - z_M(0) + \frac{1}{a}\right)^2 = -\frac{1}{a^2}, \quad z_M > z_M(0)$$

- The coordinates (τ, z) in which the observer is static is the Rindler coordinates

$$t_M = \left(z + \frac{1}{a}\right)\sinh(a\tau),$$
$$z_M = \left(z + \frac{1}{a}\right)\cosh(a\tau) + z_M(0) - \frac{1}{a}.$$

$$\Downarrow$$

$$ds^2 = dt_M^2 - dz_M^2 = (1+az)^2 d\tau^2 - dz^2$$

$$\Downarrow \quad t = a\tau, \quad \xi = z + 1/a$$

$$ds^2 = \xi^2 dt^2 - d\xi^2$$

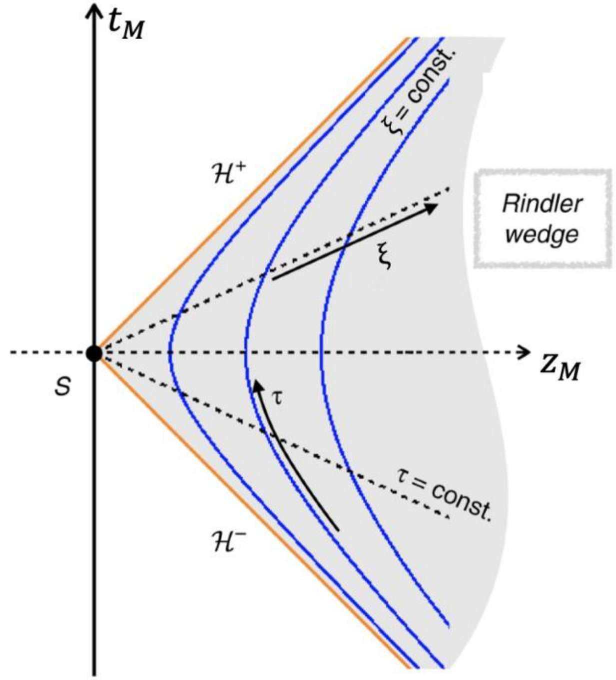

Observer at $\xi = 1/a$ has proper acceleration a

Euclidean Rindler coordinates and Unruh temperature

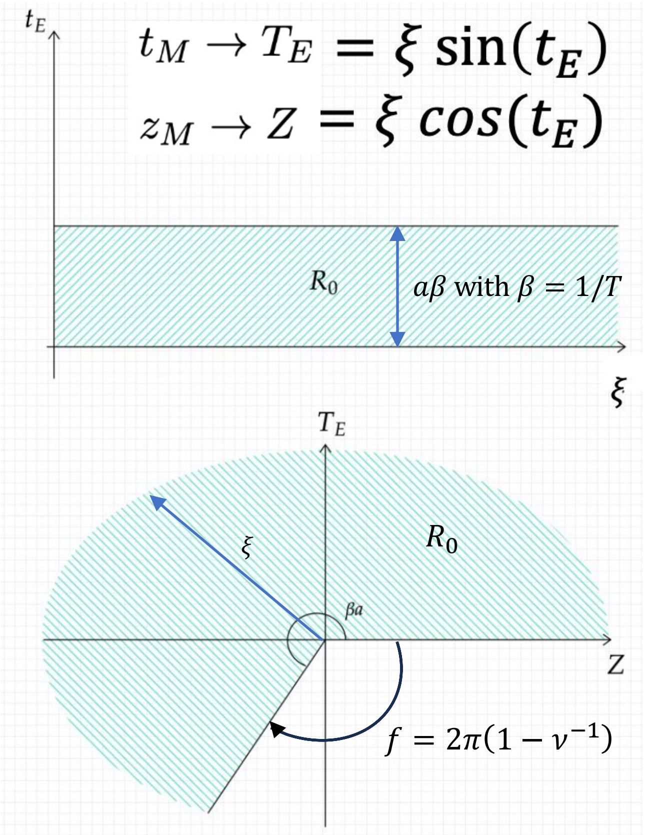

Euclidean Rinder coordinates at finite temperature T is a cone with deficit angle $f = 2\pi(1 - \nu^{-1})$ with $\nu = \frac{2\pi T}{a} = T/T_U$. To avoid a negative f, we need $T > T_U$

$$T_U = \frac{a}{2\pi} \quad : \text{Unruh temperature}$$

Identify $t_E = 0$ and $t_E = a\beta$

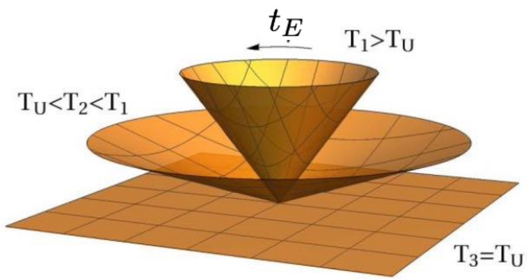

- Unruh temperature is not only geometric, it is the temperature of Minkowski vacuum seen by accelerating observer (Unruh effect)

Nonlinear sigma model analysis

- The model

$$\mathcal{L}_{NL\sigma M} = -\frac{1}{2}\Phi^T \Box \Phi - M_\pi^2 f_\pi \sigma, \qquad \Phi^T = (\pi^a, \sigma) \qquad \Phi^T\Phi = f_\pi^2.$$

- Effective action

$$\Gamma[\sigma,\lambda] = \int \mathrm{d}^4x \left(-\frac{1}{2}\sigma\Box\sigma + \frac{\lambda}{2}(\sigma^2 - f_\pi^2) + \frac{N}{2}\ln\frac{-\Box+\lambda}{-\Box} - M_\pi^2 f_\pi \sigma \right)$$

- Gap equations

$$\frac{\delta\Gamma}{\delta\sigma} = -\Box\sigma + \lambda\sigma - M_\pi^2 f_\pi = 0,$$
$$\frac{\delta\Gamma}{\delta\lambda} = \frac{\sigma^2 - f_\pi^2}{2} + \frac{N}{2}\underline{G(x,x;\lambda)} = 0,$$

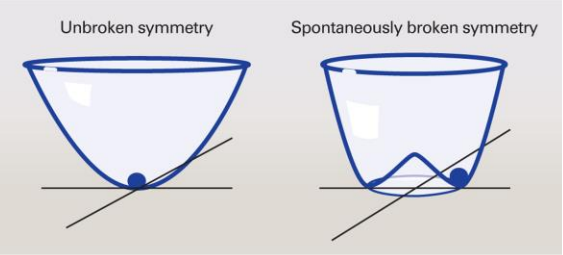

- Field operator and Green function (propagator)

$$\hat{\phi} = \int_0^\infty \mathrm{d}\omega \int \frac{\mathrm{d}^2\mathbf{k}}{2\pi}\sqrt{\frac{\sinh\pi\omega}{\pi^2}} K_{i\omega}(m_\perp\xi)(\hat{a}_{\omega,k}\mathrm{e}^{-i\omega t + i\mathbf{k}\cdot\mathbf{x}} + \hat{a}^\dagger_{\omega,k}\mathrm{e}^{i\omega t - i\mathbf{k}\cdot\mathbf{x}}) \Rightarrow G(x,x') = i\langle 0_R|T\phi(x)\phi(x')|0_R\rangle.$$

Nonlinear sigma model analysis

- Extend it to Euclidean time

$$G_E(x_E, x'_E) = \int_0^\infty \mathrm{d}\omega \int \frac{\mathrm{d}^2\mathbf{k}}{(2\pi)^2} \frac{\sinh \pi\omega}{\pi^2} K_{i\omega}(m_\perp \xi) K_{i\omega}(m_\perp \xi') e^{-\omega|t_E - t'_E| + i\mathbf{k}\cdot(\mathbf{x}-\mathbf{x}')},$$

- Extend it to finite temperature

$$G_\nu(t_E, t'_E) = G_\nu(t_E + \beta_R, t'_E) \text{ where } \beta_R = 1/T_R = a/T \text{ and } \nu = 2\pi T/a$$

$$\begin{aligned} G_\nu(x_E, x'_E) &= \sum_n G_E(t_E - t'_E + \beta_R n) \\ &= \int_0^\infty \mathrm{d}\omega \int \frac{\mathrm{d}^2\mathbf{k}}{(2\pi)^2} \frac{\cosh \omega(|t_E - t'_E| - \beta_R/2)}{\sinh(\beta_R \omega/2)} \frac{\sinh \pi\omega}{\pi^2} K_{i\omega}(m_\perp \xi) K_{i\omega}(m_\perp \xi') \mathrm{e}^{i\mathbf{k}\cdot(\mathbf{x}-\mathbf{x}')} \end{aligned}$$

- Gap equation at chiral limit

$$\sigma^2 = f_\pi^2 - N G_\nu(x_E, x_E; 0)$$

- There is divergence in the above one-loop result: vacuum contribution

Nonlinear sigma model analysis

- What vacuum contribution to subtract?

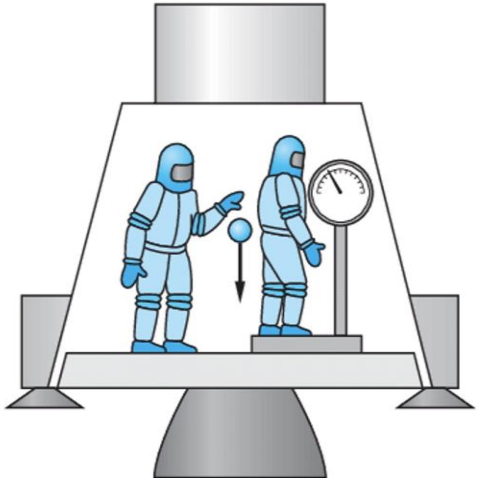

Minkowski vacuum

$$a_k^M|0_M\rangle = 0,$$

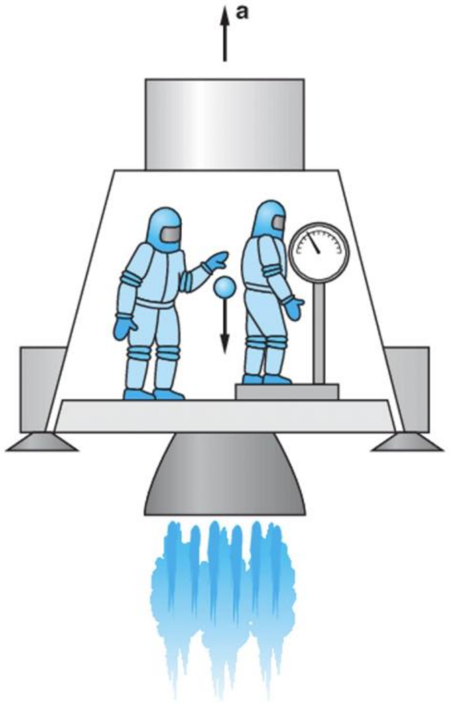

Rindler vacuum

$$a_k^R|0_R\rangle = 0$$

Nonlinear sigma model analysis

- What vacuum contribution to subtract?

Minkowski vacuum

$$a_k^M|0_M\rangle = 0,$$

Rindler vacuum

$$a_k^R|0_R\rangle = 0$$

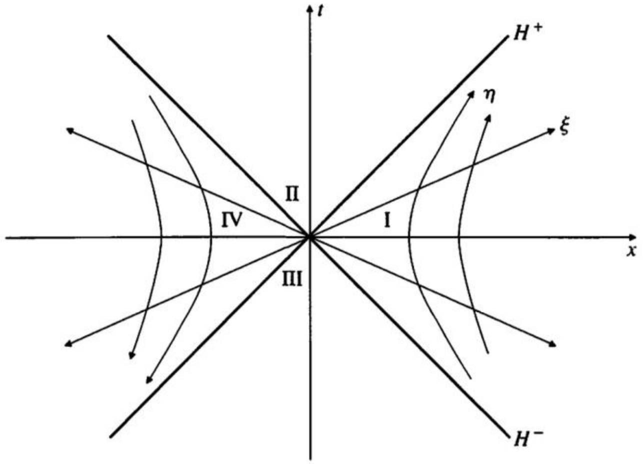

- Related by a Bogoliubov transformation

$$a_k^R = \left[2\sinh\left(\frac{\pi\omega}{a}\right)\right]^{-1/2}\left(e^{\pi\omega/2a}a_k^{(1)M} + e^{-\pi\omega/2a}a_{-k}^{(2)M\dagger}\right)$$

- Perhaps the most profound difference is Unruh effect

$$\langle 0_M|a_k^{R\dagger}a_k^R\rangle 0_M\rangle = \frac{1}{e^{\omega/T_U}-1} \qquad T_U = \frac{a}{2\pi}$$

Nonlinear sigma model analysis

- Subtraction with respect to the Minkowski vacuum

$$a_k^M|0_M\rangle = 0,$$

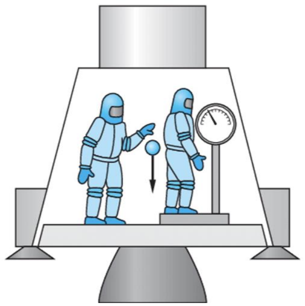

$$\sigma^2 = f_\pi^2 - \frac{1}{(a\xi)^2}\frac{N}{12}\left(T^2 - \frac{a^2}{(2\pi)^2}\right)$$

Local observer with constant acceleration a: $\xi = 1/a$

$$T_c(a) = \sqrt{\frac{12 f_\pi^2}{N} + (\frac{a}{2\pi})^2} = \sqrt{T_{c0}^2 + (\frac{a}{2\pi})^2}.$$

- Subtraction with respect to the Rindler vacuum

$$a_k^R|0_R\rangle = 0$$

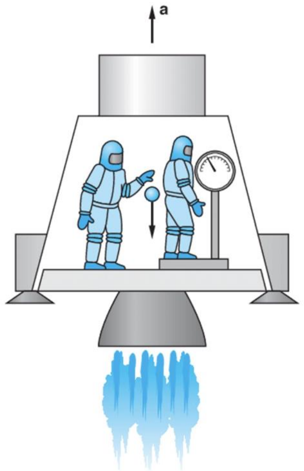

$$\sigma^2 = f_\pi^2 - \frac{T^2}{a^2\xi^2}\frac{N}{12}$$

Local observer with constant acceleration a: $\xi = 1/a$

$$T_c(a) = \sqrt{\frac{12 f_\pi^2}{N}} = T_{c0}$$

Nonlinear sigma model analysis: phase diagram

- Subtraction with respect to the Minkowski vacuum

$$a_k^M|0_M\rangle = 0$$

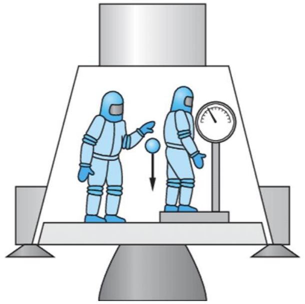

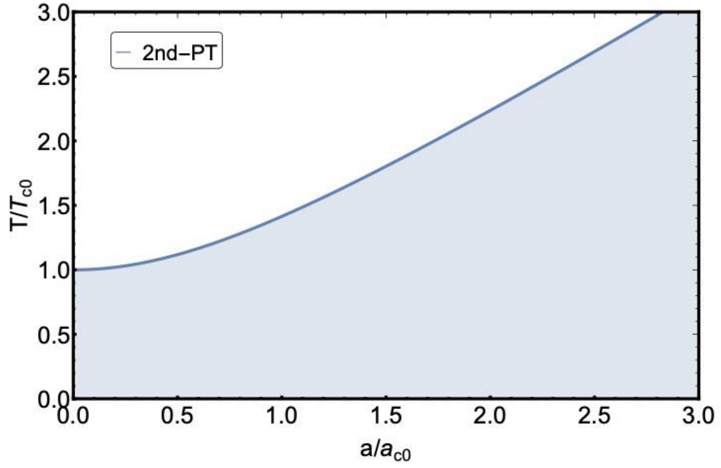

(see also Chernodub 2025)

- Subtraction with respect to the Rindler vacuum

$$a_k^R|0_R\rangle = 0$$

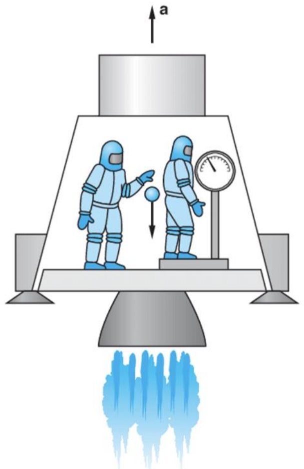

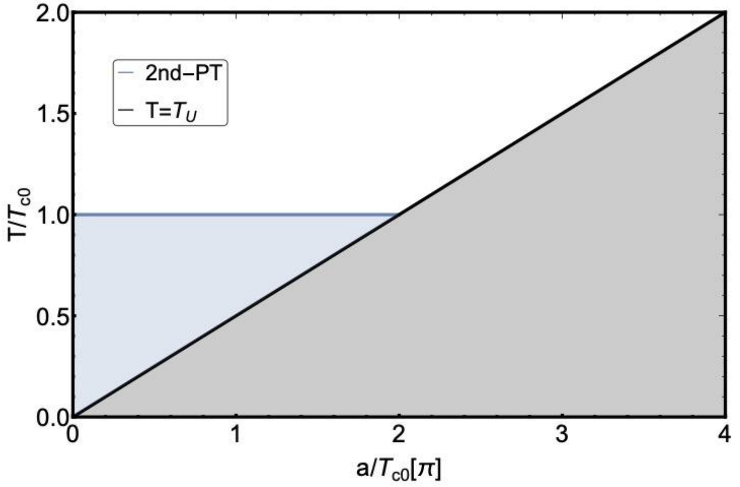

(Zhu-Chen-XGH, to appear)

Nonlinear sigma model analysis: phase diagram

- Calculation is just calculation, but which one accelerating observer really sees?
- Perhaps the one with respect to the Rindler vacuum is more reasonable

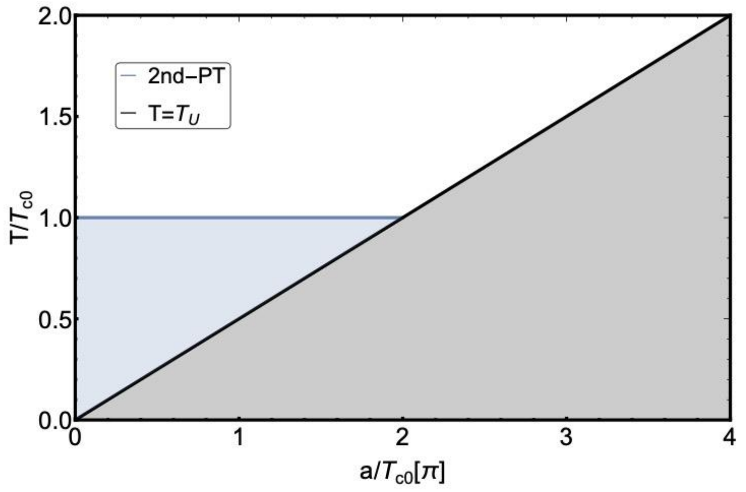

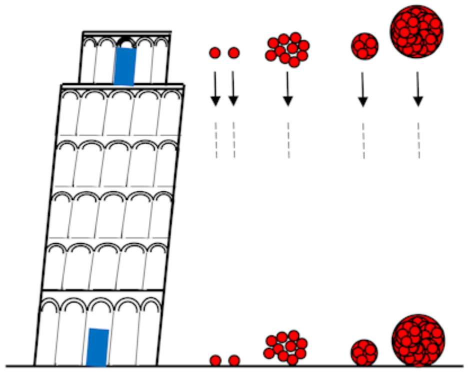

$$G(x,x') = i\langle 0_R|T\phi(x)\phi(x')|0_R\rangle,$$

$$G_M(x,x') = i\langle 0_M|T\phi(x)\phi(x')|0_M\rangle$$

Equivalence principle: Local experiments in a free-falling frame give the same results as in inertial frame

NJL model analysis

- Let us go into more micro degree of freedom by considering NJL for quarks

$$\mathcal{L}_{NJL} = \bar{\psi}\left[i\gamma^\mu \nabla_\mu - m_0\right]\psi + \frac{G_\pi}{2}\left[(\bar{\psi}\psi)^2 + \left(\bar{\psi}i\gamma^5\psi\right)^2\right]$$

- Gap equation

$$\frac{m - m_0}{G_\pi} = i\,\mathrm{Tr}(S), \qquad S(x, x') = (\hat{D} + m)G(x, x'),$$

- Euclidean Green function (propagator)

$$G_E(x_E, x'_E) = \int_0^\infty \mathrm{d}\omega \int \frac{\mathrm{d}^2\mathbf{k}}{(2\pi)^2} \frac{\sinh \pi(\omega + i\gamma^{\hat{0}}\gamma^{\hat{3}}/2)}{\pi^2} K_{i\omega-\gamma^{\hat{0}}\gamma^{\hat{3}}/2}(m_\perp \xi) K_{i\omega-\gamma^{\hat{0}}\gamma^{\hat{3}}/2}(m_\perp \xi') e^{-\omega|t_E - t'_E| + i\mathbf{k}\cdot(\mathbf{x}-\mathbf{x}')}$$

- Extend it to finite temperature

$$\begin{aligned} G_\nu &= \sum_n (-1)^n G_E(t_E - t'_E + \beta_R n) \\ &= \int_0^\infty \mathrm{d}\omega \int \frac{\mathrm{d}^2\mathbf{k}}{(2\pi)^2} \frac{\sinh(\beta_R\omega/2 - \omega|t_E - t'_E|)}{\cosh(\beta_R\omega/2)} \frac{\sinh \pi(\omega + i\gamma^{\hat{0}}\gamma^{\hat{3}}/2)}{\pi^2} K_{i\omega-\gamma^{\hat{0}}\gamma^{\hat{3}}/2}(m_\perp \xi) K_{i\omega-\gamma^{\hat{0}}\gamma^{\hat{3}}/2}(m_\perp \xi') e^{i\mathbf{k}\cdot(\mathbf{x}-\mathbf{x}')}. \end{aligned}$$

NJL model analysis

- Subtraction with respect to the Minkowski vacuum

$$a_k^M|0_M\rangle = 0,$$

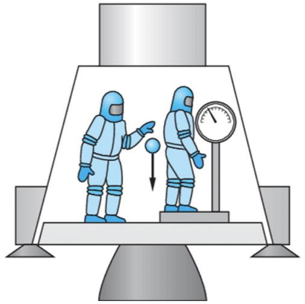

Local observer with constant acceleration a: $\xi = 1/a$

$$T_c(a) = \sqrt{\frac{3\Lambda^2}{\pi^2} - \frac{6}{G} + \frac{a^2}{(2\pi)^2}} = \sqrt{T_{c0}^2 + \left(\frac{a}{2\pi}\right)^2},$$

- Subtraction with respect to the Rindler vacuum

$$a_k^R|0_R\rangle = 0$$

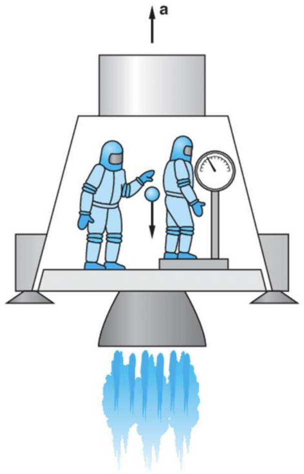

Local observer with constant acceleration a: $\xi = 1/a$

$$T_c(a) = \sqrt{\frac{3\Lambda^2}{\pi^2} - \frac{6}{G_\pi}} = T_{c0}$$

NJL model analysis

- The phase diagram is completely consistent with NLsM analysis

$$a_k^M|0_M\rangle = 0,$$

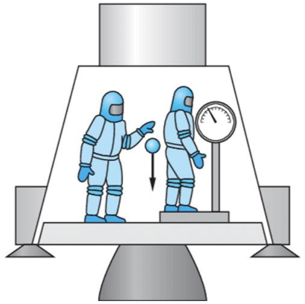

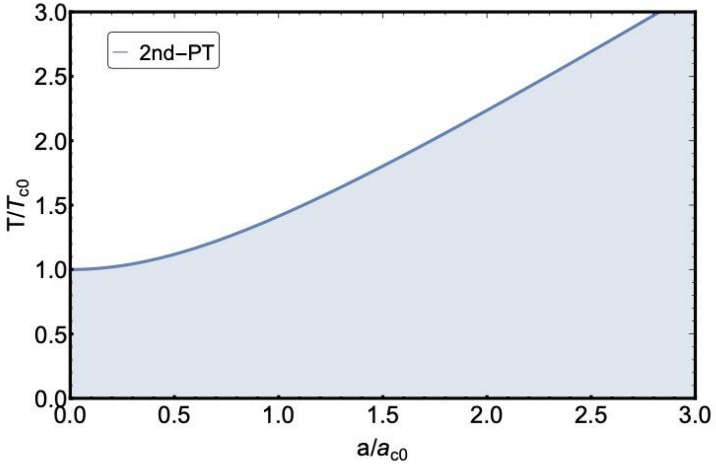

(see also Chernodub 2025)

- The phase diagram is completely consistent with NLsM analysis

$$a_k^R|0_R\rangle = 0$$

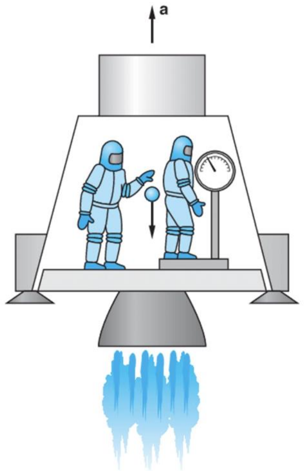

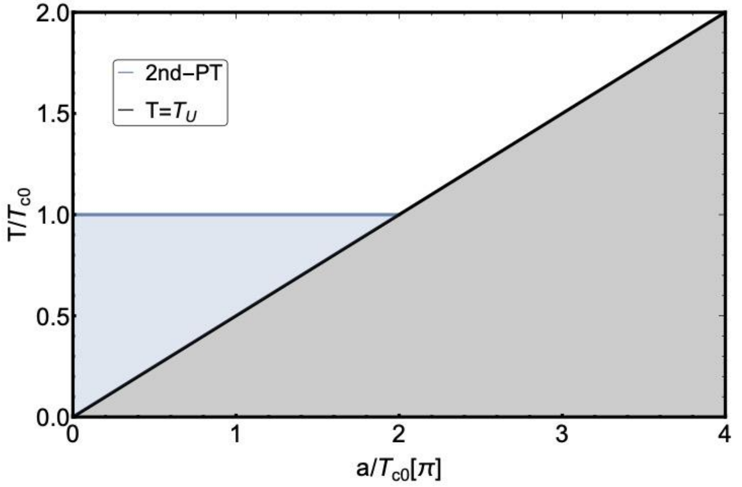

(Zhu-Chen-XGH, to appear)

Lattice formulation

- Formulate lattice action in the following accelerating metric

$$g_{\mu\nu} = \begin{pmatrix} (1+gz)^2 & 0 & 0 & 0 \\ 0 & -1 & 0 & 0 \\ 0 & 0 & -1 & 0 \\ 0 & 0 & 0 & -1 \end{pmatrix}$$

$$S_G^{lat} = \frac{\beta}{N_c} \sum_n \left\{ (1+gz) \sum_{i<j<4} \mathrm{Retr}\left[1 - \bar{U}_{ij}^2\right] + \sum_{i=1,2,3} \frac{\mathrm{Retr}\left[1 - \bar{U}_{4i}^2\right]}{1+gz} \right\}$$

$$S_F^{lat} = \sum_{n,n'} \bar{\chi}(n) D \chi(n'),$$

$$D_F = \left\{ \sum_{i=x,y,z} \sum_{\Delta_i = \pm i} (1+g\bar{z}) \eta_{\Delta_i}(n) U_{\Delta_i}(n) \delta_{n,n'-\delta_i} + \eta_\tau(n) \left(U_\tau(n) \delta_{n,n'-\tau} - U_{-\tau}(n) \delta_{n,n'+\tau} \right) \right.$$
$$\left. + \frac{g}{2} \eta_z(n) \left(U_z(n) \delta_{n,n'-z} + U_{-z}(n) \delta_{n,n'+z} \right) + 2(1+gz) a m \delta_{n,n'} \right\}$$

= $+\frac{1}{2} g \gamma_3^E$ → Sign problem

Lattice results

- Measurements are done at quenched limit

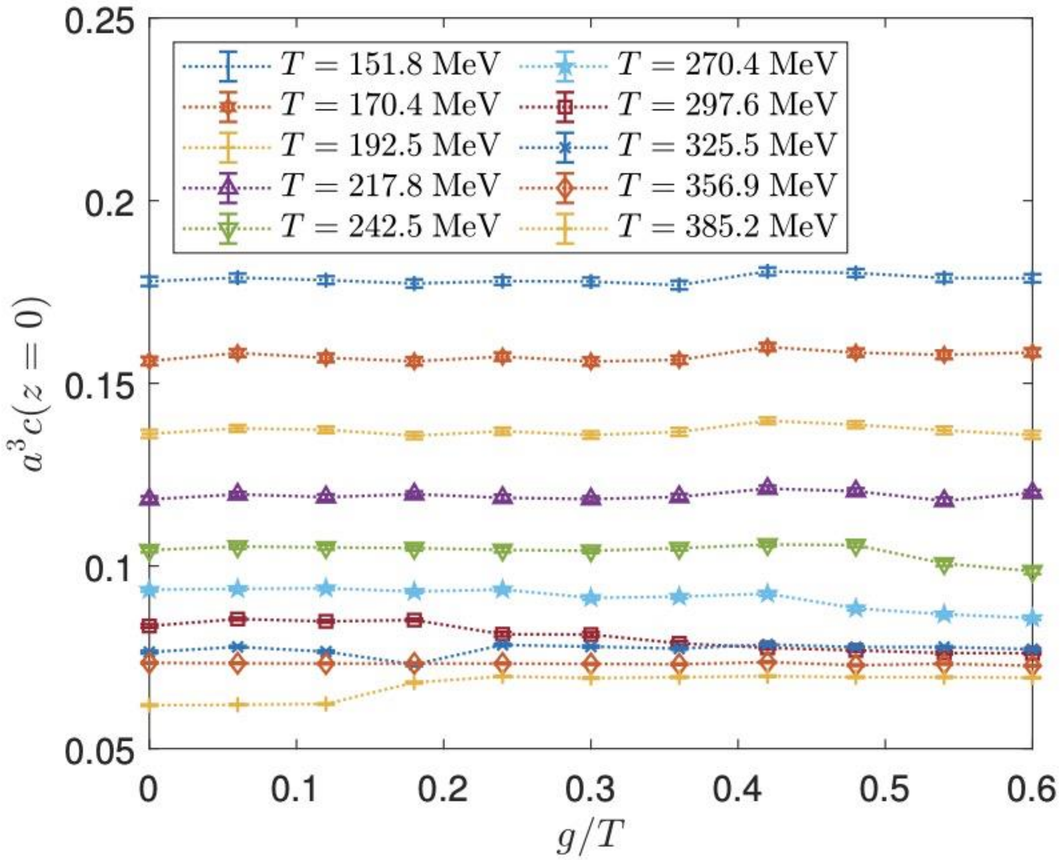

Chiral condensate vs acceleration g

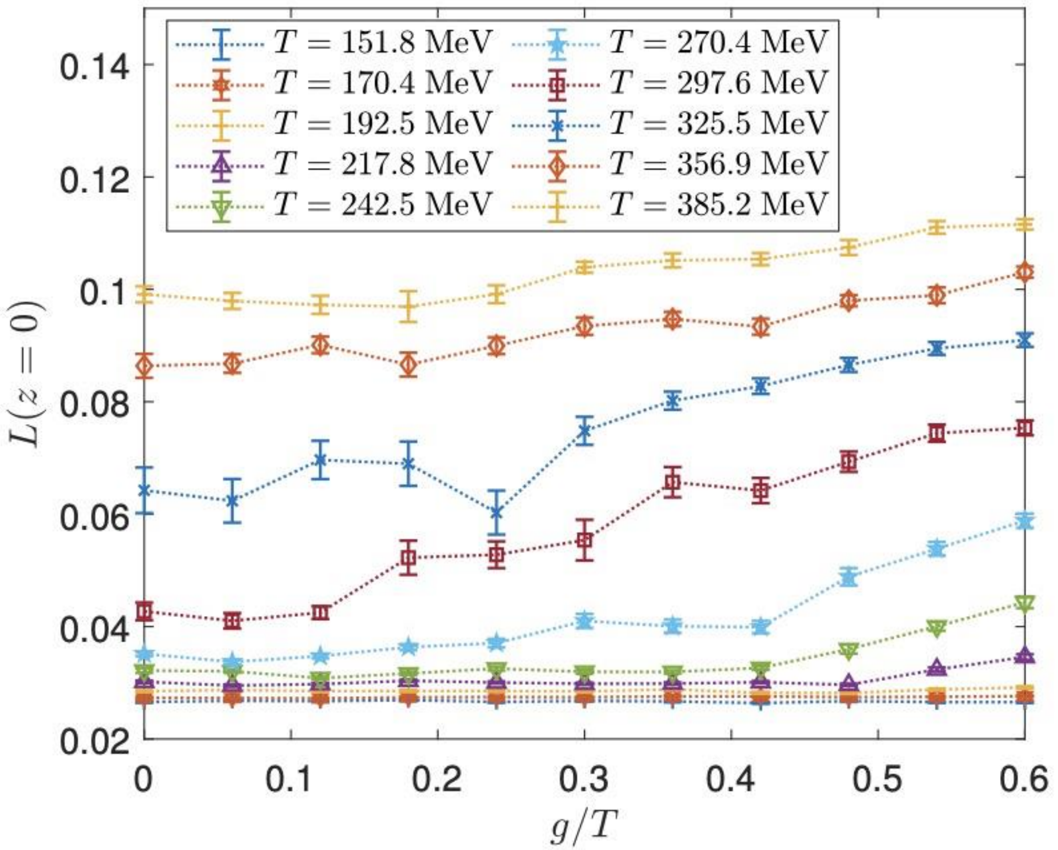

Polyakov loop vs acceleration g

(Yang-XGH, to appear)

No acceleration dependence measured

Lattice results

- A recent simulation for pure Yang-Mills

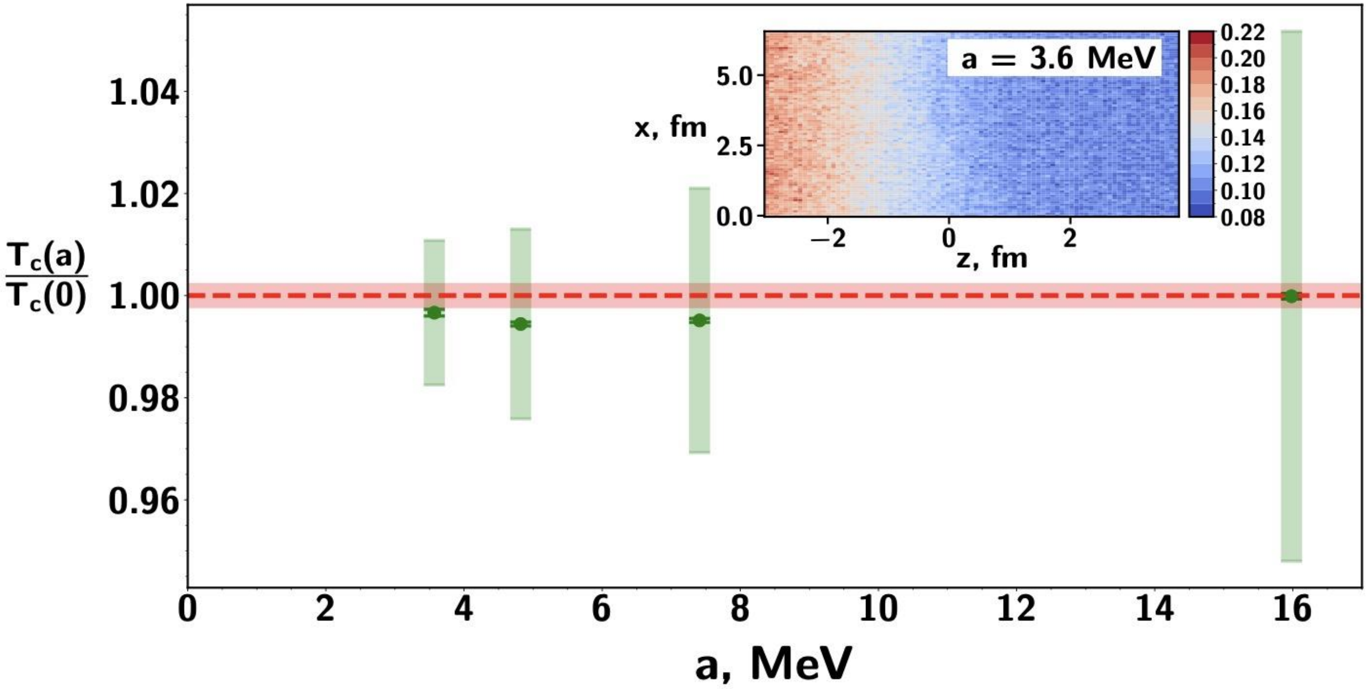

Deconfinment temperature as determined by Polyakov loop

(Braguta etal 2024)

No acceleration dependence measured

Summary and outlooks

Summary and outlooks

- It is NOT understood how rotation modifies chiral phase transitions.
- Acceleration effects depends crucially on subtraction scheme
- Outlooks:
  - More lattice simulations
  - Cross check torsion effect on chiral condensate and confinement on lattice

    (Yamamoto 2020)
  - Complex Langevin method

    (Azuma-Morita-Yoshida 2023)
  - fRG or DSE for accelerating-rotating QCD
  - More model studies
  - … …

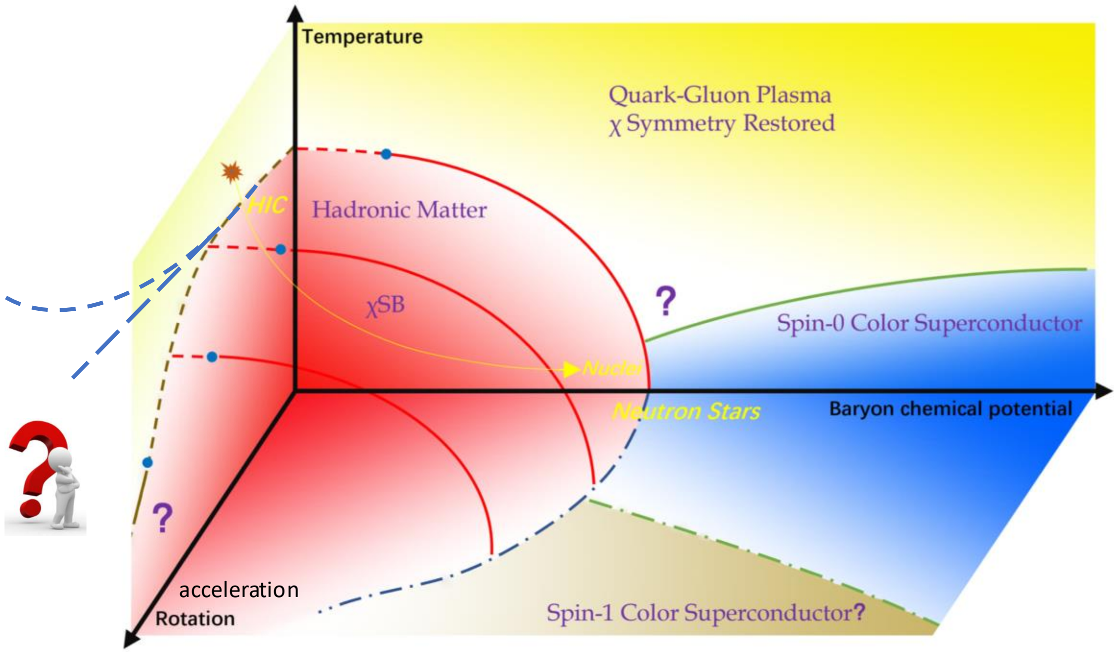

Thank you!

Where rotating quark matter: Quark-gluon plasma

- From global angular momentum to vorticity to hyperon spin polarization

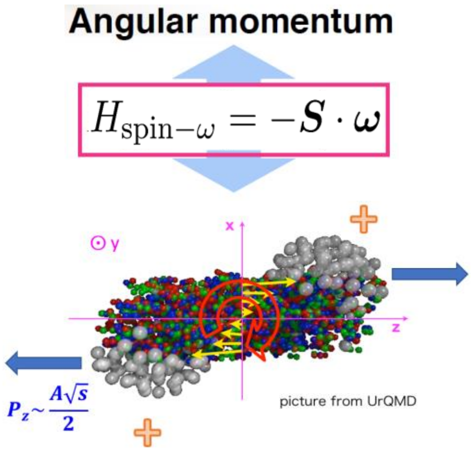

(at thermal equilibrium)

$$\frac{dN_s}{d\boldsymbol{p}} \sim e^{-(H_0 - \boldsymbol{\omega}\cdot\boldsymbol{S})/T}$$

$$\mathrm{P} = \frac{N_\uparrow - N_\downarrow}{N_\uparrow + N_\downarrow} \sim \frac{\omega}{2T}$$

- First measurement of Λ polarization by STAR@RHIC *

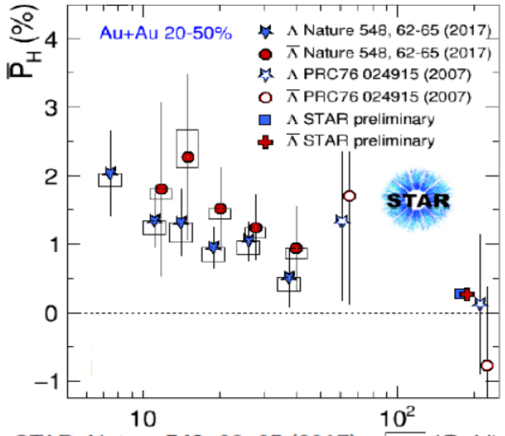

STAR, Nature **548**, 62–65 (2017)

parity-violating decay of hyperons

In case of Λ's decay, daughter proton preferentially decays in the direction of Λ's spin (opposite for anti-Λ)

$$\frac{dN}{d\Omega^*} = \frac{1}{4\pi}(1 + \alpha \mathbf{P_\Lambda}\cdot\mathbf{p_p^*})$$

α: Λ decay parameter (α_Λ=0.732)
P_Λ: Λ polarization
p_p^*: proton momentum in Λ rest frame

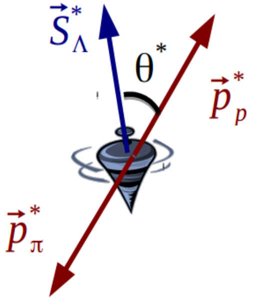

$\Lambda \to p + \pi^-$
(BR: 63.9%, cτ ~7.9 cm)

(* First theoretical proposal: Liang and Wang 2004, later by Voloshin 2004)

Where rotating quark matter: Quark-gluon plasma

- More recent measurements: Ξ^-, Ω^- by STAR@RHIC, Λ by ALICE@LHC

STAR, PRL126, 162301 (2021)

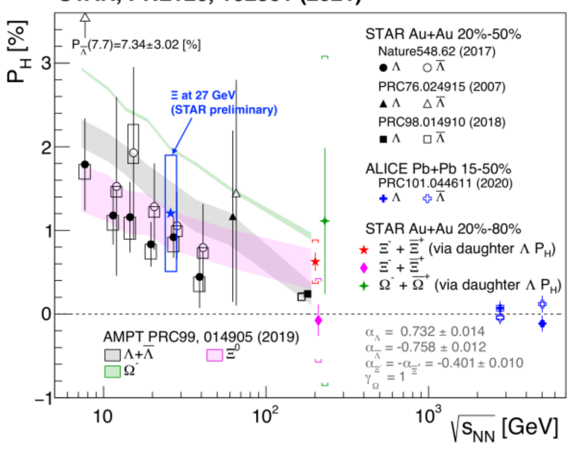

hyperon	decay mode	α_H	magnetic moment μ_H	spin
Λ (uds)	Λ→pπ⁻ (BR: 63.9%)	0.732	-0.613	1/2
Ξ⁻ (dss)	Ξ⁻→Λπ⁻ (BR: 99.9%)	-0.401	-0.6507	1/2
Ω⁻ (sss)	Ω⁻→ΛK⁻ (BR: 67.8%)	0.0157	-2.02	3/2

- Λ at low energy by STAR@RHIC 2021, HADES@GSI 2021

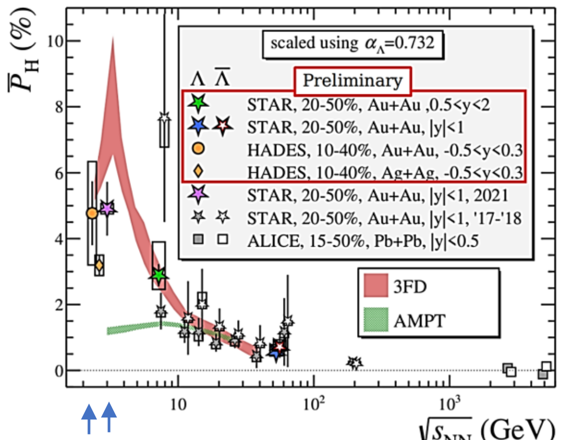

2.4, 2.55 3

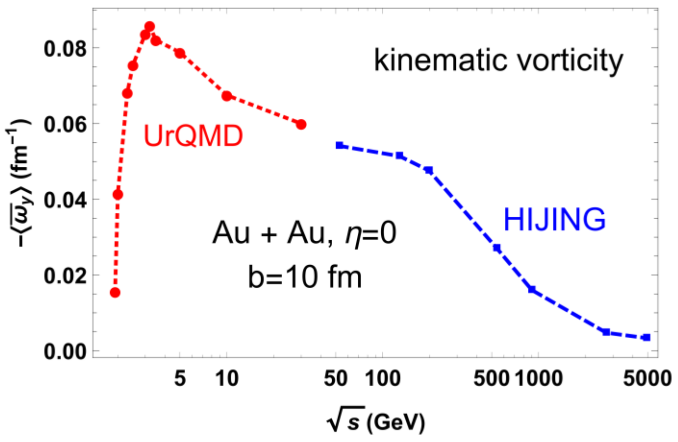

(Deng-XGH 2016, Deng-XGH-Ma-Zhang 2020)

- "The most vortical fluid": $\omega \sim 10^{20} - 10^{21} s^{-1}$
- Relativistic suppression at high energies

Rotating quark-meson model

- Purpose: beyond mean-field approximation ---- fRG approach
- Quark-meson model is perhaps the simplest model to consider

$$\mathcal{L} = \phi[-(-\partial_\tau + \Omega\hat{L}_z)^2 - \nabla^2]\phi + U(\phi) \ + \bar{q}[\gamma^0(\partial_\tau - \Omega\hat{J}_z) - i\gamma^i\partial_i + g(\sigma + i\vec{\pi}\cdot\vec{\tau}\gamma^5)]q$$

$$U(\phi) = \frac{m^2}{2}\phi^2 + \frac{\lambda}{4}\phi^4 - c\sigma \quad \text{with} \quad \phi = (\sigma, \vec{\pi})$$

- With Dirichlet B.C. for mesons and no-flux B.C. for quarks, solutions for Klein-Gordon eq. and Dirac eq.:

$$\phi = \frac{1}{N_{l,i}^2} e^{-i(\varepsilon - \Omega l)t + il\theta + ip_z z} J_l(p_{l,i} r)$$

$$u_+ = \frac{\mathrm{e}^{-i(\varepsilon-\Omega j)+ip_z z}}{\sqrt{\varepsilon+m}} \begin{pmatrix} (\varepsilon+m)\phi_l \\ 0 \\ p_z\phi_l \\ i\tilde{p}_{l,i}\varphi_l \end{pmatrix}, \quad \text{with} \quad \phi_l = \mathrm{e}^{il\theta} J_l(\tilde{p}_{l,i} r)$$

$$u_- = \frac{\mathrm{e}^{-i(\varepsilon-\Omega j)+ip_z z}}{\sqrt{\varepsilon+m}} \begin{pmatrix} 0 \\ (\varepsilon+m)\phi_l \\ -i\tilde{p}_{l,i}\varphi_l \\ -p_z\phi_l \end{pmatrix}, \qquad \varphi_l = \mathrm{e}^{i(l+1)\theta} J_{l+1}(\tilde{p}_{l,i} r)$$

Discretized momenta $p_{l,i}$ and $\tilde{p}_{l,i}$ are determined by B.C.s

Rotating quark-meson model

- The flow equation for effective action

Partition function with an IR regulator

$$Z_k[J] = \int D\chi e^{-S[\chi]+\int_x \chi(x)J(x)-\Delta S_k[\chi]}$$

regulator

$$\Delta S_k[\chi] = \frac{1}{2}\int \frac{d^d q}{(2\pi)^d}\chi^*(q)R_k(q)\chi(q)$$

Legendre transformation:

$$\Gamma_k[\phi] = -W_k[J] + \int_x \phi(x)J(x) + \Delta S_k[\phi]$$

flow equation (Wetterich 1993)

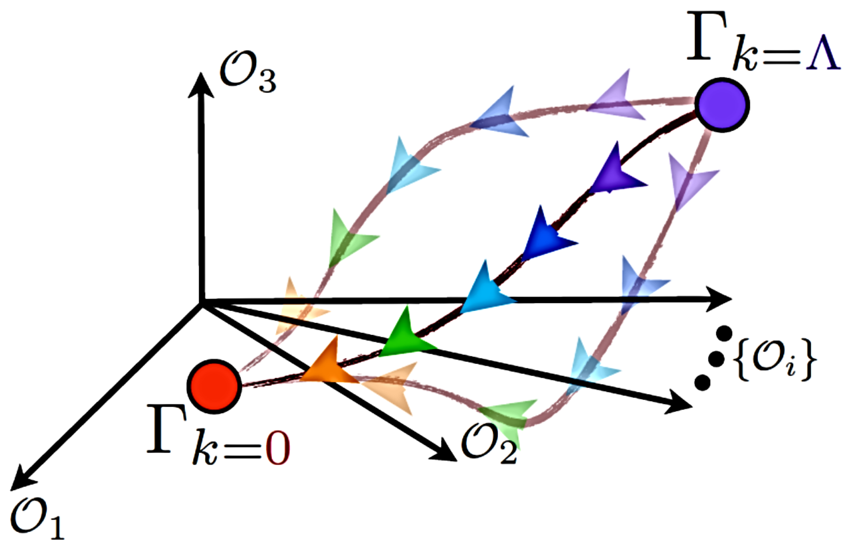

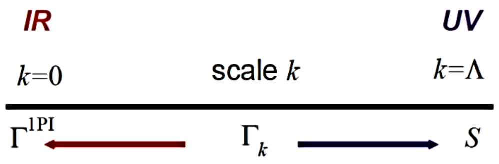

$$\partial_k\Gamma_k = \frac{1}{2}\mathrm{tr}(G_{\phi,k}\partial_k R_{\phi,k}) - \mathrm{tr}(G_{q,k}\partial_k R_{q,k})$$ with coarse-graining regulators

$$R_{\phi,k} = (k^2 - p^2)\theta(k^2 - p^2)$$

$$\hat{R}_{q,k} = -i\gamma^i\partial_i\left(\frac{k}{\sqrt{-\nabla^2}} - 1\right)\theta(k^2 + \nabla^2)$$

Rotating quark-meson model

- The flow equation for effective action

Partition function with an IR regulator

$$Z_k[J] = \int D\chi e^{-S[\chi]+\int_x \chi(x)J(x)-\Delta S_k[\chi]}$$

regulator

$$\Delta S_k[\chi] = \frac{1}{2}\int \frac{d^d q}{(2\pi)^d}\chi^*(q)R_k(q)\chi(q)$$

Legendre transformation:

$$\Gamma_k[\phi] = -W_k[J] + \int_x \phi(x)J(x) + \Delta S_k[\phi]$$

flow equation (Wetterich 1993)

$$\partial_k \Gamma_k = \frac{1}{2}\mathrm{tr}(G_{\phi,k}\partial_k R_{\phi,k}) - \mathrm{tr}(G_{q,k}\partial_k R_{q,k})$$ with propagators

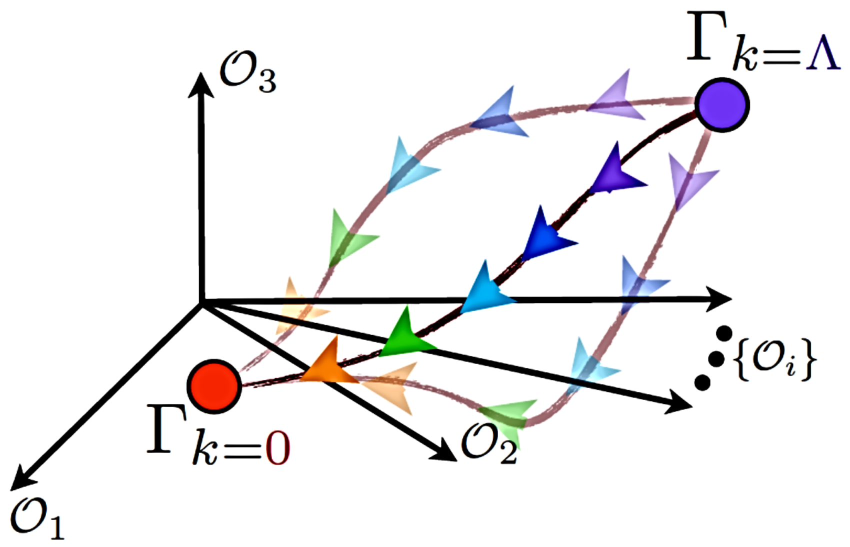

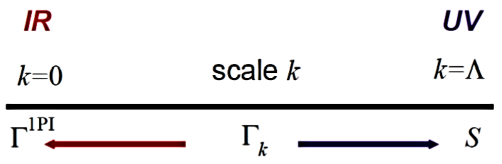

$$\hat{G}^{-1}_{\phi,k} = -(-\partial_\tau + \Omega\hat{L}_z)^2 - \nabla^2 + \hat{R}_{\phi,k} + \frac{\partial^2 U}{\partial\phi_i\partial\phi_j}$$

$$\hat{G}^{-1}_{q,k} = \gamma^0(-\partial_\tau + \Omega\hat{J}_z) - \gamma^i\partial_i + \hat{R}_{q,k} + g\phi$$

Rotating quark-meson model

- The flow equation for effective potential: Local potential approximation

$$
\begin{aligned}
\partial_k U_k &= \frac{1}{\beta V}(\partial_k \Gamma_k^B + \partial_k \Gamma_k^F), \\
&= \frac{1}{(2\pi)^2}\left\{ \sum_{l,i} \frac{1}{N_{l,i}^2} \mathrm{tr} \frac{k\sqrt{k^2 - p_{l,i}^2}}{\varepsilon_\phi} \frac{1}{2}\left[\coth\frac{\beta(\varepsilon_\phi + \Omega l)}{2} + \coth\frac{\beta(\varepsilon_\phi - \Omega l)}{2}\right] J_l(p_{l,i} r)^2 \theta(k^2 - p_{l,i}^2) \right. \\
&\quad \left. - \sum_{l,i} \frac{1}{\tilde{N}_{l,i}^2} 2N_c N_f \frac{k\sqrt{k^2 - \tilde{p}_{l,i}^2}}{\varepsilon_q} \frac{1}{2}\left[\tanh\frac{\beta(\varepsilon_q + \Omega j)}{2} + \tanh\frac{\beta(\varepsilon_q - \Omega j)}{2}\right] [J_l(\tilde{p}_{l,i} r)^2 + J_{l+1}(\tilde{p}_{l,i} r)^2] \theta(k^2 - \tilde{p}_{l,i}^2) \right\}
\end{aligned}
$$

Depend on U_k

- Solved using grid method with UV cutoff at 1 GeV; System size is 100/GeV, other parameters are fitted to non-rotating results

Rotating quark-meson model

- Chiral condensate on T-Ω plane (Chen-Zhu-XGH 2023)

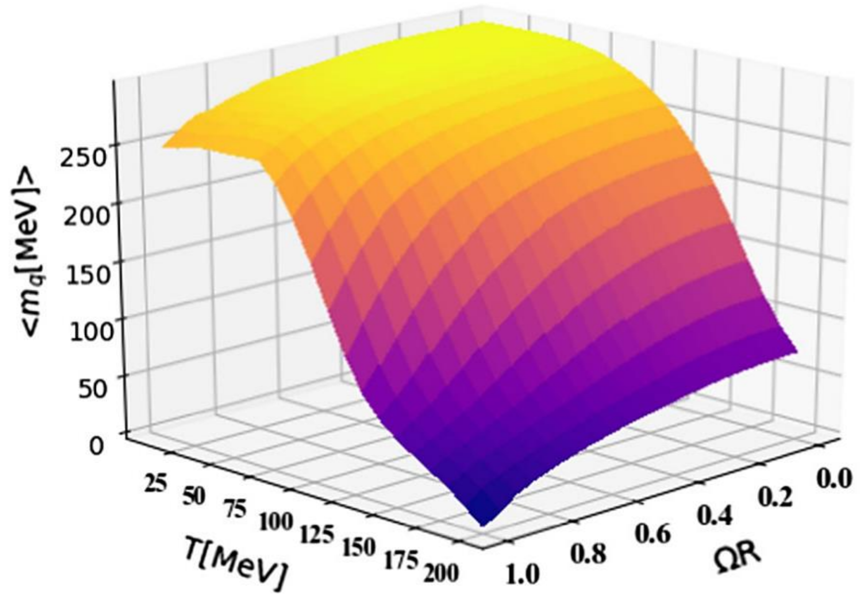

fRG calculation

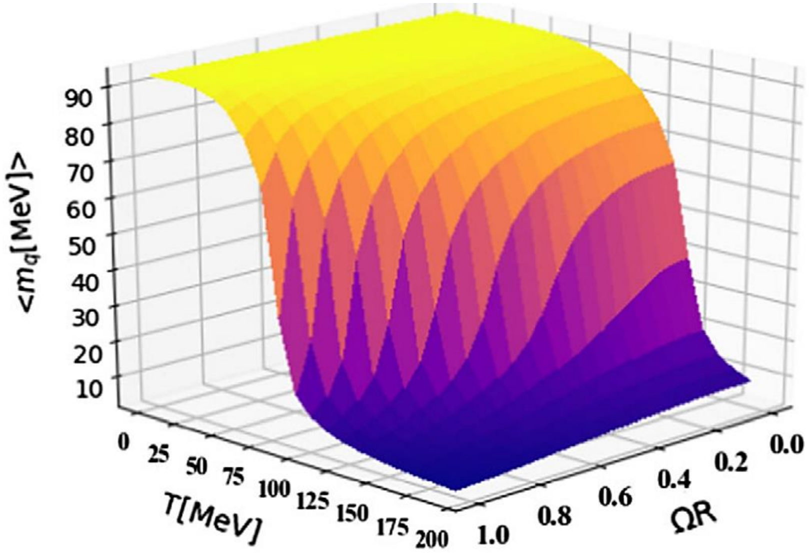

Mean-field calculation

- No surprise: Ω tends to suppress chiral condensate

Confinement under rotation

- It is not easy to intuitively imagine the rotational effect on confinement
- Argument based on hadron resonance gas (HRG) model

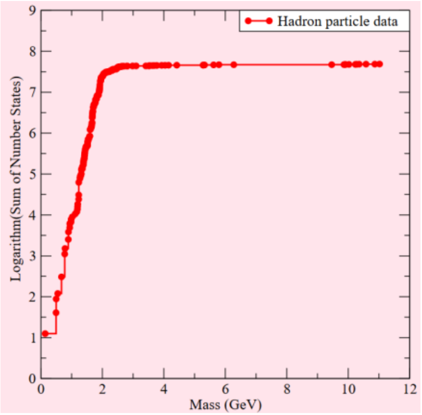

Interpreted as deconf. T

$$\rho(m) = e^{m/T_H} \Rightarrow Z = \int dm\, \rho(m)\, e^{-m/T} \Rightarrow \text{diverges for } T > \boxed{T_H}$$

Chosen to be indep. of rotation

$$\left.\begin{aligned} p(T,\mu,\omega;\Lambda) &= \sum_{m;\, M_i \le \Lambda} p_m + \sum_{b;\, M_b \le \Lambda} p_b \\ p_{\mathrm{SB}} &\equiv (N_c^2 - 1)\, p_g + N_c N_f\, (p_q + p_{\bar{q}}) \end{aligned}\right\} \quad \frac{p}{p_{\mathrm{SB}}}(T_c,\, \mu,\, \omega) = \boxed{\gamma} \Rightarrow$$

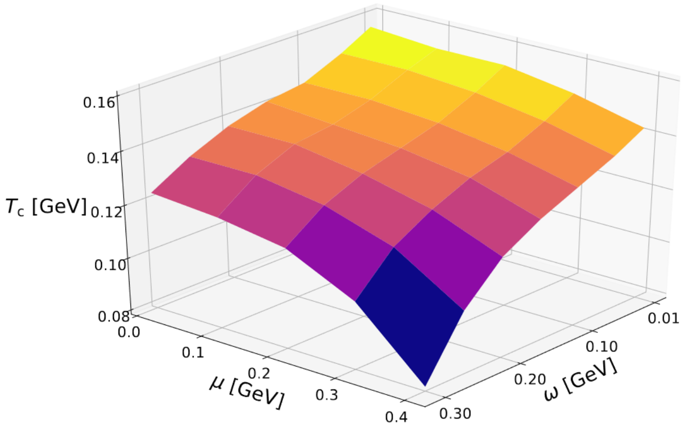

(Fujimoto-Fukushima-Hidaka 2021)

- Rotation favors deconfinement

Confinement under rotation

- It is not easy to intuitively imagine the rotational effect on confinement
- Argument based on Tolman-Ehrenfest temperature

$$\left.\begin{aligned} T(\boldsymbol{x})\sqrt{g_{00}(\boldsymbol{x})} &= T_0 \\ g_{00} &= 1 - \rho^2\Omega^2 \end{aligned}\right\} \quad T(\rho) = \frac{T(0)}{\sqrt{1-\rho^2\Omega^2}}$$

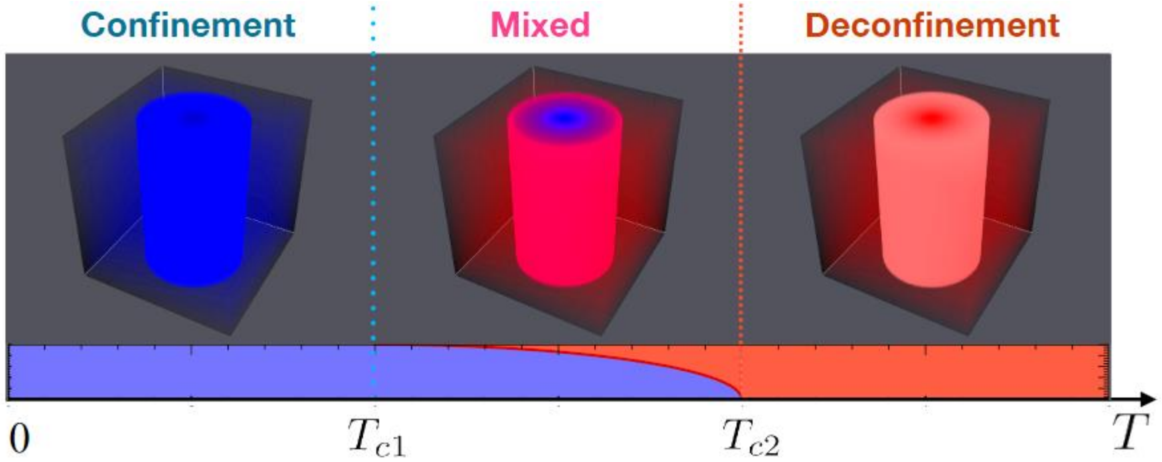

(Chernodub 2020)

- Rotation favors deconfinement

Confinement under rotation

- It is not easy to intuitively imagine the rotational effect on confinement
- Results based on holography models

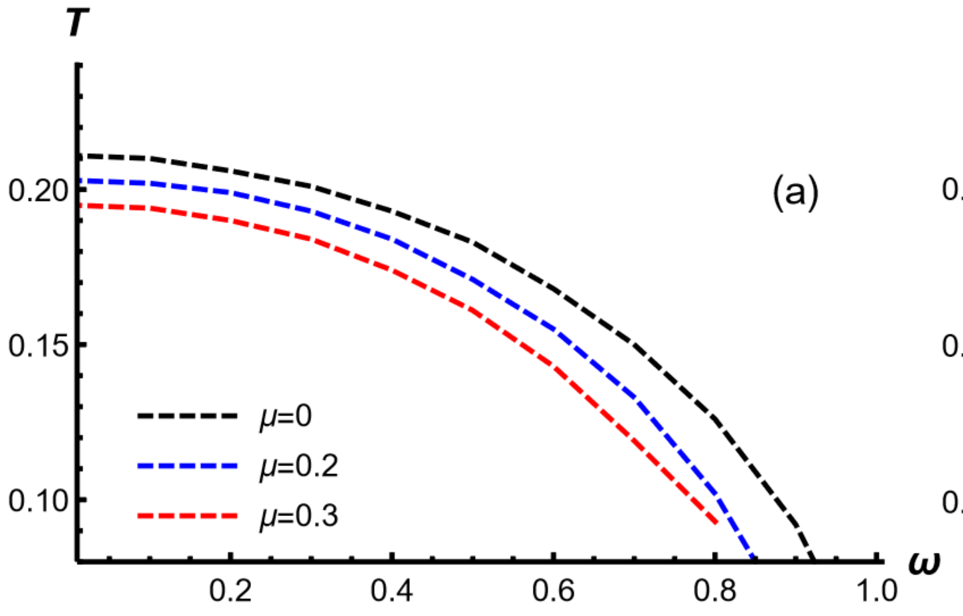

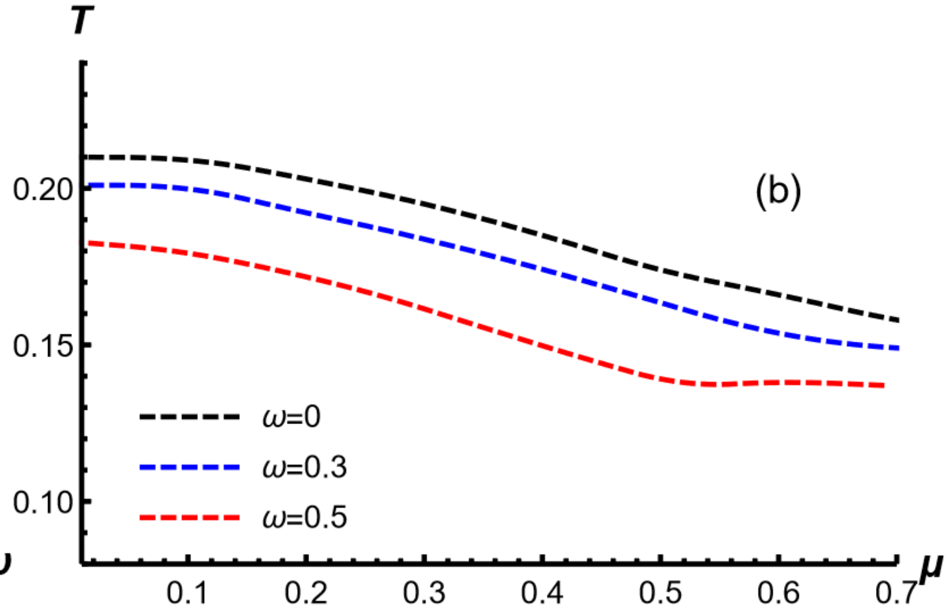

(Chen-Zhang-Li-Hou-Huang 2020)

- Rotation favors deconfinement

Formulate rotating lattice

- Gluons and Wilson fermions (Angular momentum) (Yamamoto-Hirono 2013)
- Pure gluons (Polyakov loop) (Braguta etal 2021)
- We consider gluons and 2+1 flavor staggered fermions

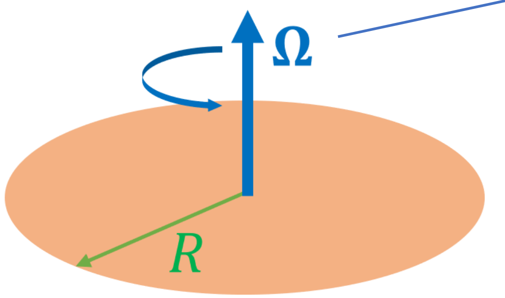

Imaginary rotation: $\boldsymbol{\Omega} \to -i\boldsymbol{\Omega}_I$

No sign problem
No causality constraint

Projective-plane B.C for x-y plane
Periodic B.C. for t and z direction

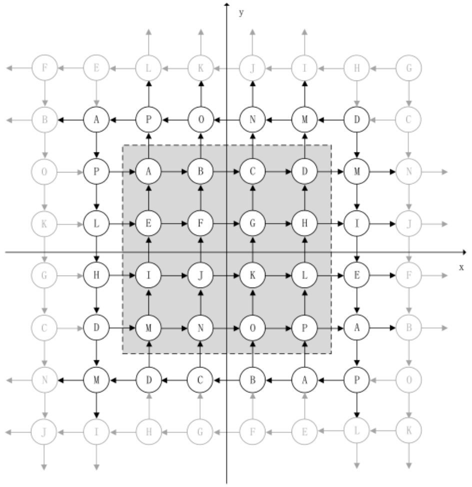

- We measure: (imaginary) angular momentum

Ji decomposition

$$\mathbf{J} = \mathbf{J}_G + \mathbf{s}_q + \mathbf{L}_q$$

$$\begin{cases} \mathbf{J}_G = \sum_a \int d^3x \, \mathbf{r} \times (\mathbf{E}^a \times \mathbf{B}^a) \, , \\ \mathbf{s}_q = \int d^3x \, q^\dagger \frac{\boldsymbol{\Sigma}}{2} q, \\ \mathbf{L}_q = \frac{1}{i} \int d^3x \, q^\dagger \mathbf{r} \times \mathbf{D} q. \end{cases}$$

Chiral vortical effect

Results of angular momentum

- Angular momentum
- J_G and L_q approximately $\propto r^2$, and s_q approximately independent of r, thus

$$\rho_J = \frac{1}{N_{taste} N_{r_{max}}} \sum_{n_x^2+n_y^2<r_{max}^2} \frac{\langle J(n) \rangle}{a\Omega (a^{-1} r)^2}$$

Moment of inertia

$$\xi_q = \frac{1}{4 N_{r_{max}}} \sum_{n_x^2+n_y^2<r_{max}^2} \frac{\langle s_q(n) \rangle}{a\Omega}$$

Quark spin susceptibility

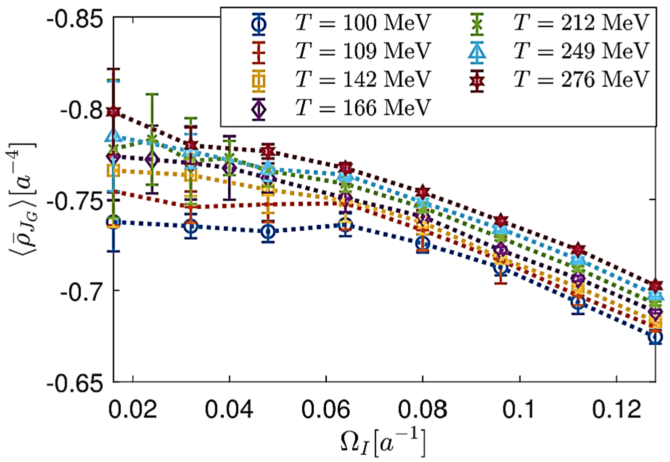

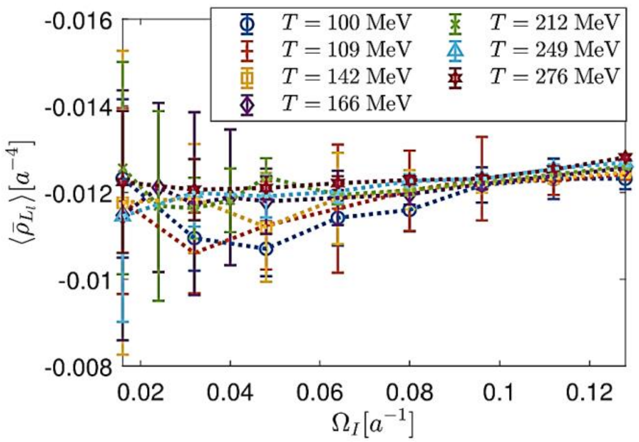

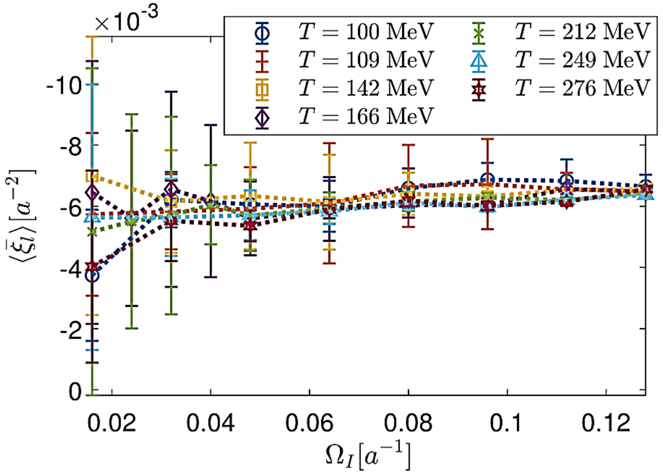

(Yang-XGH 2023)

Discussion 1: Is analytical continuation sensible?

- For unbounded system, imaginary rotation is always OK, but real rotation is not. So the analytical continuation is problematic.
- For finite system preserving causality, the analytical continuation is OK

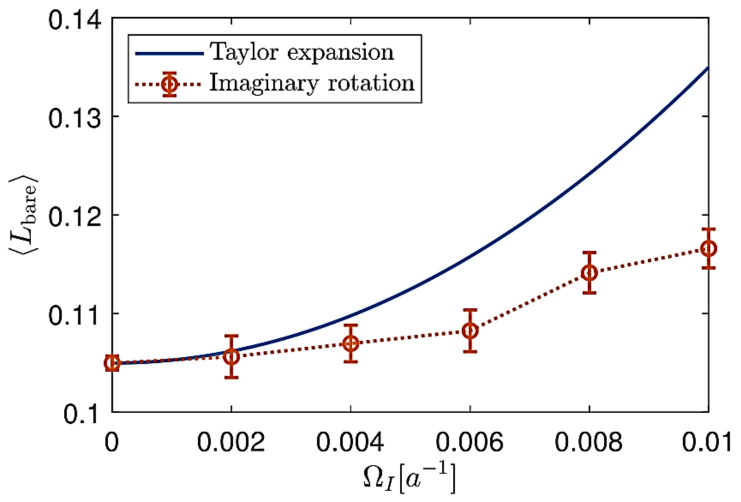

Real rotation lattice simulation using Taylor expansion

(Yang-XGH 2023)

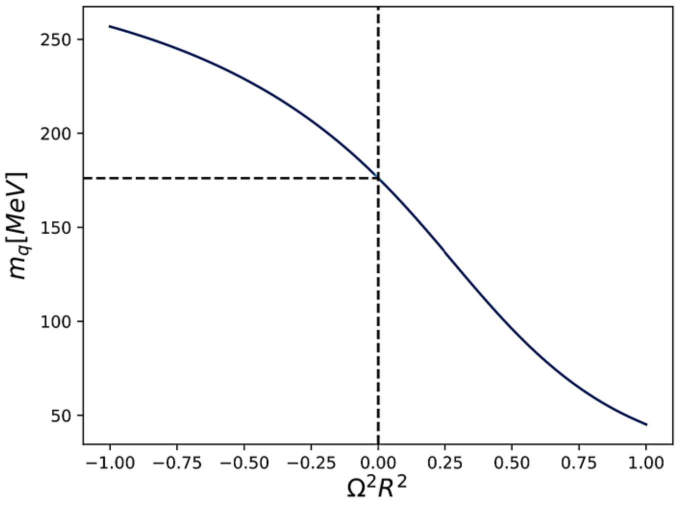

fRG with real and imaginary rotation

(Chen-Zhu-XGH 2023)

Discussion 2: Strong coupling versus weak coupling?

- It seems the lattice results depend on coupling (Yang-XGH, not published)

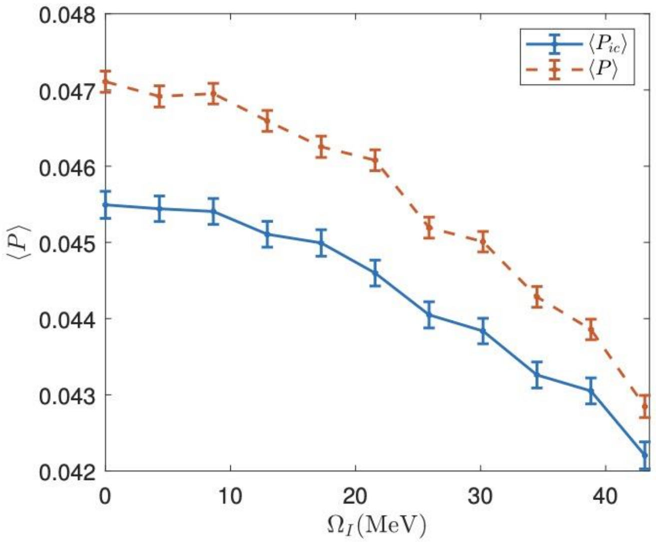

Polyakov loop at strong coupling
(Lattice coupling =2.5)

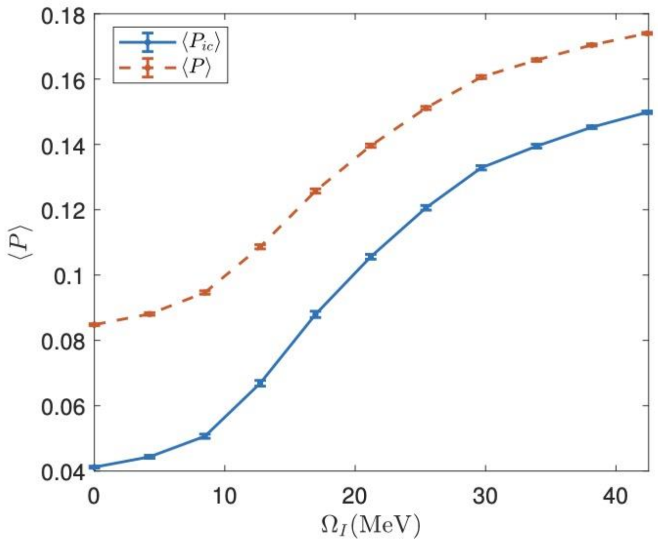

Polyakov loop at weak coupling
(Lattice coupling=5.3)

- Strong-coupling expansion applied to lattice action shows that Polyakov loop decreases (increases) with imaginary (real) rotation.

(Wang-Chen-Hou-Ren 2025, Fukushima-Shimada 2025)

Discussion 3: Vacuum does not rotate?

- Natural to expect that the perturbative vacuum does not rotate
- Is it true for QCD vacuum containing nontrivial gluon condensate?

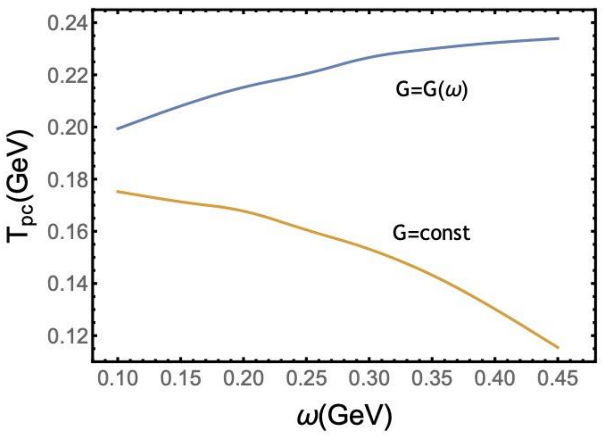

Chiral-transition T_c with rotation-dependent coupling in NJL model

(Jiang 2021)

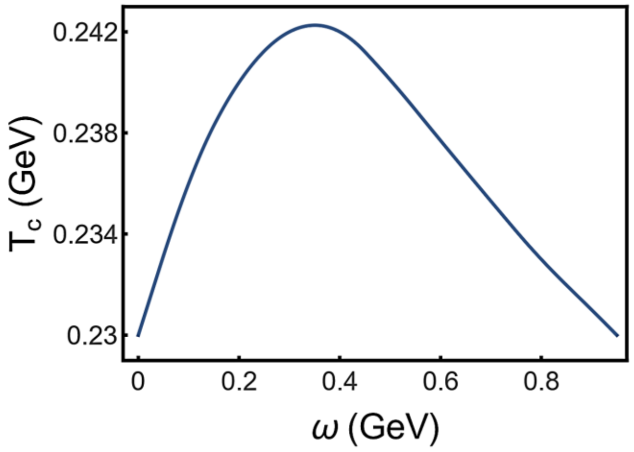

Deconfinement temperature in presence of Caloron background

(Jiang 2023)

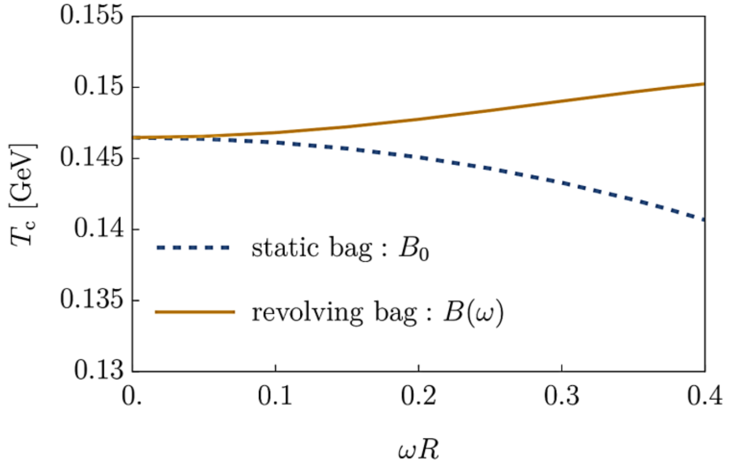

Bag constant may response to rotation and enhance the deconfinement temperature

(Mameda 2023)

Discussion 4: Important to have other nonperturbative calculations?

- fRG for rotating QCD

Gluon propagator

$$G_{\hat{\mu}\hat{\nu}}(x,x') = \sum_n \sum_l \int \frac{p_t \mathrm{d}p_t \mathrm{d}p_z}{(2\pi)^2} [\frac{1}{p_l^2}\delta^L_{\hat{\mu}\hat{\nu}} + (\frac{1}{p_{l+1}^2} + \frac{1}{p_{l-1}^2})\delta^T_{\hat{\mu}\hat{\nu}} + (\frac{1}{p_{l+1}^2} - \frac{1}{p_{l-1}^2}) S_{z\hat{\mu}\hat{\nu}}] \mathrm{e}^{i\omega_n \Delta\tau + il\Delta\theta + ip_z\Delta z} J_l(p_T r) J_l(p_T r')$$

3 vertex can be handled

$$\int_0^\infty J_{n_1}(k_1\rho) J_{n_2}(k_2\rho) J_{n_3}(k_3\rho)\rho\, d\rho$$
$$= \frac{\Delta}{6\pi A}[\cos(n_1\alpha_2 - n_2\alpha_1) + \cos(n_2\alpha_3 - n_3\alpha_2) + \cos(n_3\alpha_1 - n_1\alpha_3)]$$

4 vertex is difficult

$$\int r\mathrm{d}r J_{l_1}(p_{1t}r) J_{l_2}(p_{2t}r) J_{l_3}(p_{3t}r) J_{l_4}(p_{4t}r)\delta(l_1+l_2+l_3+l_4) \;=?$$

Unruh effect and Unruh temperature

- The most famous effect of acceleration is the Unruh effect

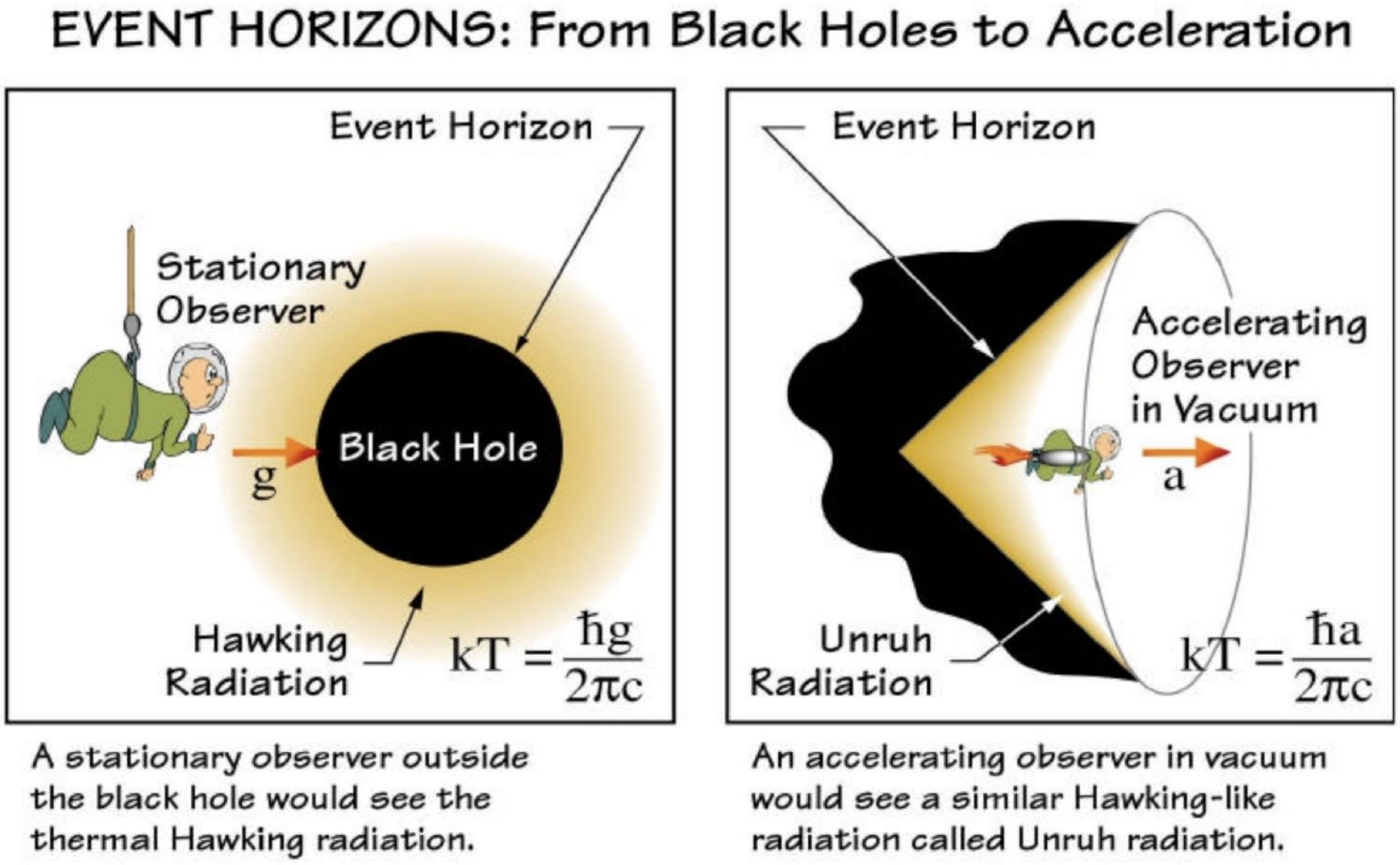

(Figure from Pisin Chen 2014)